*Human Molecular Genetics, 2008, Vol. 17, No. 3* ***440–457***
*doi:10.1093/hmg/ddm322*
*Advance Access published on November 5, 2007*

# Genomic and functional profiling of human Down syndrome neural progenitors implicates S100B and aquaporin 4 in cell injury

**Giuseppe Esposito[1], Jaime Imitola[2], Jie Lu[5], Daniele De Filippis[6], Caterina Scuderi[1], Vijay S. Ganesh[5], Rebecca Folkerth[3], Jonathan Hecht[4], Soojung Shin[7], Teresa Iuvone[6], Jonathan Chesnut[7], Luca Steardo[1] and Volney Sheen[5,*]**

[1]Department of Human Physiology and Pharmacology, 'Vittorio Erspamer' Faculty of Pharmacy, University of Rome 'La Sapienza', Rome, Italy, [2]Center for Neurologic Diseases, Division of Neurology, Brigham and Women's Hospital, Harvard Medical School, Boston MA 02115 USA, [3]Department of Pathology, Division of Neuropathology, Brigham and Women's Hospital, Harvard Medical School, Boston MA 02114 USA, [4]Department of Neuropathology, Beth Israel Deaconess Medical Center, Harvard Medical School, Boston, MA 02115, USA, [5]Department of Neurology, Beth Israel Deaconess Medical Center, Harvard Medical School, Boston, MA 02115, USA, [6]Department of Experimental Pharmacology, Faculty of Pharmacy, University Federico II of Naples Via Domenico Montesano 49, 80131 Rome, Italy and [7]Invitrogen, Carlsbad, CA 92008, USA

Received August 8, 2007; Revised and Accepted November 1, 2007

**Down syndrome (DS) is caused by trisomy of chromosome 21 and is characterized by mental retardation, seizures and premature Alzheimer's disease. To examine neuropathological mechanisms giving rise to this disorder, we generated multiple human DS neural progenitor cell (NPC) lines from the 19–21 week frontal cortex and characterized their genomic and functional properties. Microarray profiling of DS progenitors indicated that increased levels of gene expression were not limited to chromosome 21, suggesting that increased expression of genes on chromosome 21 altered transcriptional regulation of a subset of genes throughout the entire genome. Moreover, many transcriptionally dysregulated genes were involved in cell death and oxidative stress. Network analyses suggested that upregulated expression of chromosome 21 genes such as S100B and amyloid precursor protein activated the stress response kinase pathways, and furthermore, could be linked to upregulation of the water channel aquaporin 4 (AQP4). We further demonstrate in DS NPCs that S100B is constitutively overexpressed, that overexpression leads to increased reactive oxygen species (ROS) formation and activation of stress response kinases, and that activation of this pathway results in compensatory AQP4 expression. In addition, AQP4 expression could be induced by direct exposure to ROS, and siRNA inhibition of AQP4 resulted in elevated levels of ROS following S100B exposure. Finally, elevated levels of S100B-induced ROS and loss of AQP4 expression led to increased programmed cell death. These findings suggest that dysregulation of chromosome 21 genes in DS neural progenitors leads to increased ROS and thereby alters transcriptional regulation of cytoprotective, non-chromosome 21 genes in response to ongoing cellular insults.**

## INTRODUCTION

Numerous studies have demonstrated the ability to expand pluripotent human embryonic stem cells (hESCs) or more restricted multipotent human neural progenitor cells (hNPCs) and direct their differentiation into various neuronal phenotypes (1–5). These neural progenitors can undergo the same migratory pathway as endogenous precursors. They are able to integrate into the parenchyma. They also assume neuronal and glial

*To whom correspondence should be addressed. Tel: +1 6176672699; Fax: +1 6176670800; Email: vsheen@bidmc.harvard.edu

phenotypes appropriate for the region of engraftment, if transplanted during the period of developmental neurogenesis (3,6). Some studies have subsequently developed models of human central nervous system (CNS) disorders by deriving hNPCs from diseased tissues, while other studies have proposed developing models of human diseases using various manipulations of hESCs (7–10). These models are thought to be of particular benefit, when animal models do not clearly reflect the human phenotype as in Parkinson's disease, Alzheimer's disease (AD) or in Down syndrome (DS). Although such studies have raised the potential for using human reagents in the study of human diseases, few studies to date have actually sought to identify and examine potential aberrant pathways that could contribute to the disease phenotypes.

DS (OMIM 190685) is a common genetic variation caused by a duplication of chromosome 21 (8,11,12). The most profound neurological features of DS include mental retardation, seizures and early onset Alzheimer disease. DS brains weigh less than age-matched normal brains. They demonstrate simplified gyral patterning. The neuronal density and lamination are also reduced in the DS brain (13–15). Furthermore, there appears to be a preferential loss in GABA-ergic neurons and the neuronal density, while normal in early gestation, decreases later in gestation (>23 weeks) (16). Finally, the developing DS cortical neurons have shorter dendrites, fewer dendritic spines and abnormal dendritic morphology (17,18). Taken in sum, these observations are consistent with alterations in cell fate or reduced proliferation in neuronal subpopulations. Subsequent impairments in neuronal differentiation also appear to be reflected in DS brain. However, the subset of genes which are constitutively overexpressed on chromosome 21 and lead to these impairments are not known.

Analyses of DS neurons or neural progenitor cells (NPCs) in culture have allowed for characterization of some candidate, disease-causing genes in this disorder. Primary cortical neurons from gestational 16–18 week fetal DS brain fail to survive long-term in comparison to normal cultures, even in the presence of serum with survival factors (19). The neurons are more vulnerable to intracellular reactive oxygen species (ROS), in part due to mitochondrial dysfunction in DS neural cells, causing aberrant processing of amyloid precursor protein (APP). The impairment in APP processing results in increased neuronal cell death (20). More recent studies have also begun to examine renewable neural progenitors derived from DS individuals (21). Differential display PCR used on NPCs from gestational 17–19 week fetal tissue showed that SCG10, a neuron-specific growth-associated protein regulated by the neuron-restrictive silencer factor REST, was almost undetectable in the DS sample. While specific genes have been implicated in DS neural development, the underlying molecular pathways that contribute to the increased neuronal cell death and decreased neuronogenesis are not entirely clear.

To pursue molecular mechanisms contributing to the DS phenotype, we generated multiple human DS neural precursor lines, derived from the frontal cortex and examined their gene expression profiles and functional characteristics. Microarray profiling of these DS cells demonstrated upregulation of genes, located both on and off of chromosome 21. The altered gene expressions strongly implicated genes involved in cell death and oxidative stress. Network analyses suggested that overexpression of genes such as S100B and APP on chromosome 21 led to activation of stress response kinases, generation of ROS and compensatory upregulation of the water channel aquaporin 4 (AQP4) within DS NPCs. Furthermore, functional data presented here indicate that upregulation of AQP4 may serve to mitigate cell damage and death due to S100B induction of ROS. Overall, these studies provide some of the first evidence of altered molecular pathways in contributing to the DS neurologic phenotype.

## RESULTS

### Characterization of human DS NPCs

To generate human neural precursor cell lines, progenitors were isolated from the cerebral wall of the frontal cortex of 19–21 week postmortem fetuses with DS. Clonal populations were obtained from single cells, isolated by dissociation from the subventricular zone of the frontal cortex, passaged through a cell strainer, diluted to low density and then allowed to grow into multiple neurospheres. On gross observation, the DS NPCs appeared to proliferate more slowly compared with control at early time points after dissociation (NPC diameter for DS = 77 ± 9 μM, control = 125 ± 9 μM from three independent lines each within one month). To exclude potential mosaicism within individual samples, we performed fluorescent *in situ* hybridization (50/50 cells analyzed from each of three independent samples) demonstrating the additional chromosome 21 copy in metaphase and non-dividing interphase (Supplementary Fig. S1A). Gene expression profiling and culture studies were performed on three independent DS fetal brain and three independent age-matched control neural precursors obtained at gestational weeks 19–21 and cultured for no more than five passages. Examination of mRNA expression levels with the DS critical region (~3400 kb region on 21q22) revealed, on average, a 1.5-fold increase in expression of genes in this region for DS as compared to control progenitors (Supplementary Fig. S1B).

To better define the characteristics of the control and DS NPCs, we performed several levels of analyses. Pairwise comparisons of the expression levels for the ~54 000 probes in the HU133 plus 2.0 Affymetrix microarray showed a high correlation on inter-control and inter-DS comparisons, indicating that the progenitor cells were fairly uniform in their expression profiles. Moreover, significant differences were seen on control–DS sample comparison, suggesting the presence of dysregulated gene pathways in the DS precursors (Fig. 1A). Within the control and DS cell lines, we also analyzed the expression levels of multiple genes responsible for self-renewal and neural progenitor identity (Fig. 1B). The expression and conservation of this subset of genes were related to their intrinsic capacities such as self-renewal capacity and help characterize these cells as progenitors (22,23). No significant differences in the levels of expression between DS and wild-type (WT) control were seen in the transcription factors SOX2, NCOR2, ITGB1 and NEK6, which are associated with NPC self-renewal capacity (23–26). In addition, the expression of neural progenitor genes FLNA, FOXG1B and DCX (27–29) was not significantly changed.

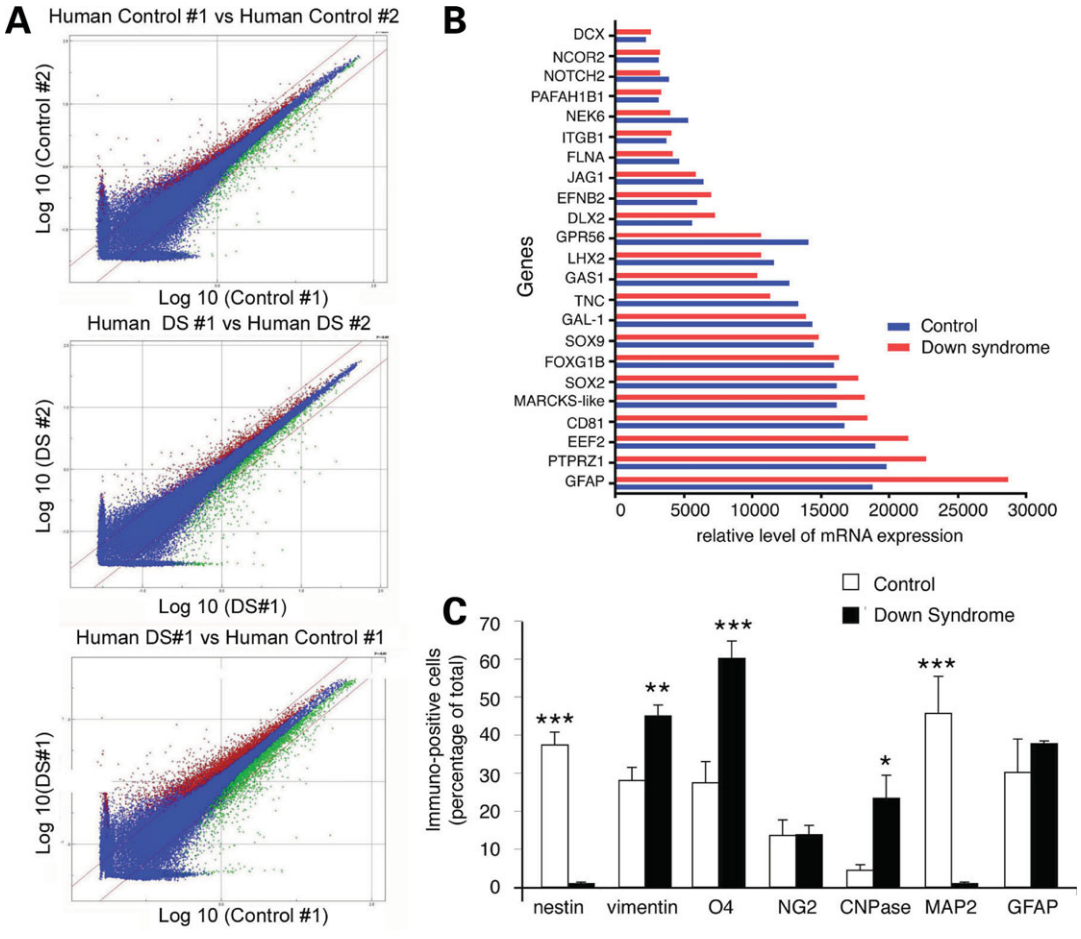


**Figure 1.** Human Down syndrome neural stem cells represent a fairly homogeneous cell population on inter-sample comparison, but differ significantly on comparison with age-matched normal controls. (**A**) Homogeneity of mRNA expression in DS and control human neural progenitors. Pairwise comparisons are performed between levels of expression for each of the 50K transcripts on the Affymetrix H133+ Array. Significant increases (red) or decreases (green) in expression are noted on comparison of a DS neural cell line versus a human control neural line (bottom graph). The high degrees of similarity on comparison between control-control (top graph) and DS-DS (middle graph) neural lines are indicated by the relatively small regions of increased (red) or decreased (green) gene expression. These observations suggest that the neural precursor cell lines derived from different individuals are fairly uniform and that the differences seen in the DS lines are likely attributable to the disease process. (**B**) Human DS neural stem cells preserve core expression of neural progenitors genes. Microarray profiling of mRNA expression comparing the expression of core NPC and progenitor genes demonstrate a non-statistical significance difference between DS NPCs and controls. Note that the only gene with a significant increase was GFAP (averaged between $n = 3$ control and $n = 3$ DS lines). (**C**) Quantitative summary of immunostaining of the three DS and three control NPC lines with regards to various neural, neuronal and glial markers. The DS progenitors exhibit increased expression for glial precursor markers including vimentin, CNPase and GFAP, suggesting a predominant glial progenitor phenotype. Fluorescent photomicrograph images of representative immunostaining patterns are shown in Figure 2. $^{*}P < 0.01$; $^{**}P < 0.005$; $^{***}P < 0.002$.

However, we found a slight increase in the expression of GFAP in DS progenitors compared with controls. GFAP is an intermediate filament protein gene, that is, expressed in hNPCs and mature astrocytes (30,31). Several of the genes involved in cancer and cell proliferation (PTPRZ1 and EEF2) were also increased in DS NPCs, which generally showed increased rates of proliferation with serial passaging. These data suggested that while DS neural progenitors were fairly uniform between human samples and largely retained the core features of gene expression seen in neural progenitors.

As initial comparisons on the microarray platform raised the possibility that the DS progenitors shared similarities with glial progenitor phenotypes, we performed cell-type-specific marker analysis of the undifferentiated NPCs by immunostaining to further characterize the identity of these NPCs (Figs 1C and 2). Although both the control and DS progenitors were age-matched, isolated from the same regions of the brain and cultured under the same conditions, the DS progenitors from each of the three independent DS lines exhibited increased expression for glial phenotypes, including vimentin (radial glia), glial fibrillary acid protein (astrocytes/NPCs), O4 sulfatide (oligodendrocyte progenitors) and 2′,3′-cyclic nucleotide 3′-phosphodiesterase (oligodendrocytes). No significant difference was observed in NG2 chondroitin sulfate proteoglycan (oligodendrocyte precursors/NPCs), whereas control NPCs showed increased expression of nestin (neuroepithelial precursors) and MAP2 (neurons). Thus, while the DS NPCs retained progenitor characteristics and could express neuronal markers, they also appeared to adopt skewed glial progenitor phenotypes compared with control.

To address whether the differences seen in the DS as opposed to control progenitors reflected differences due to maturation

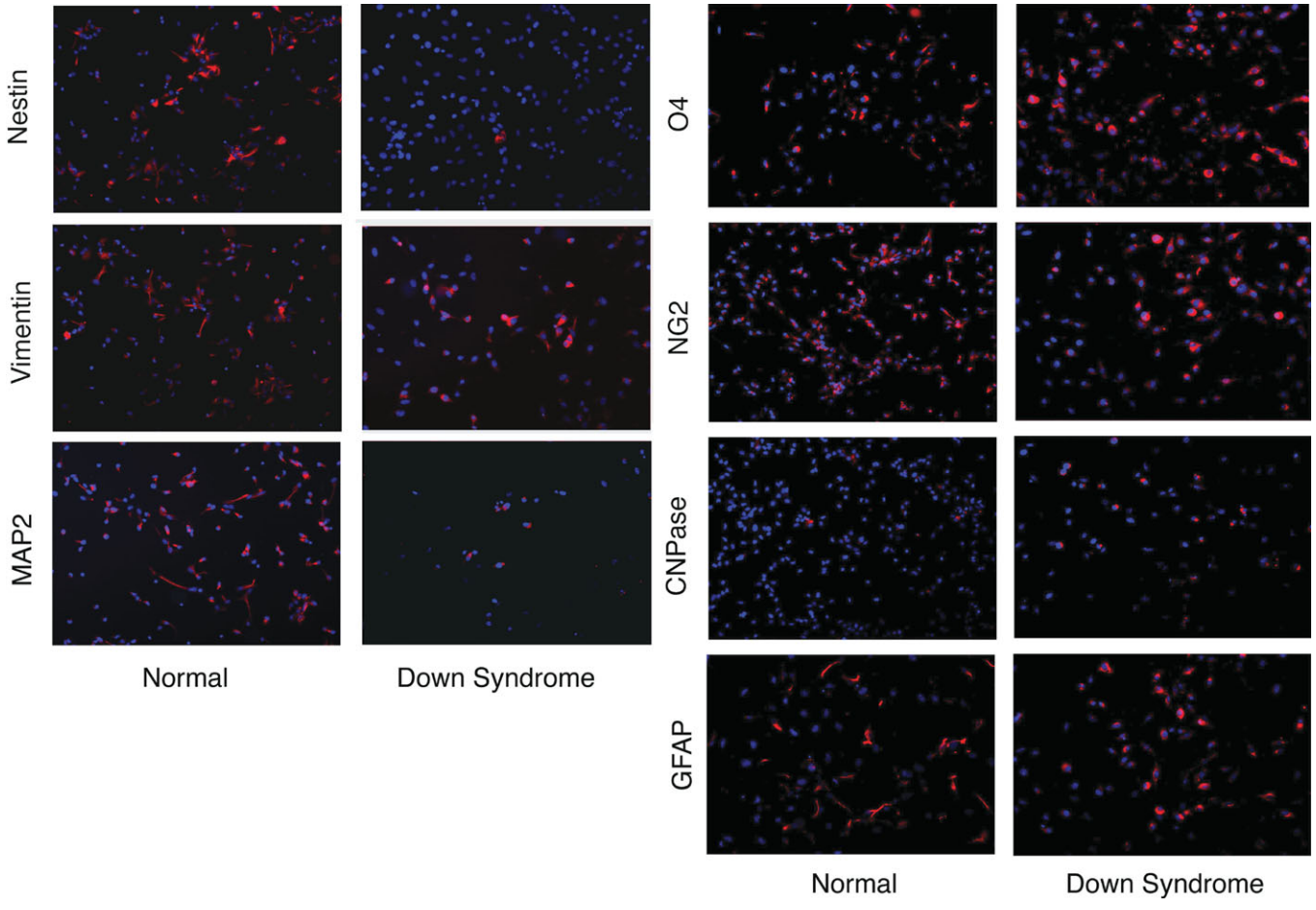


**Figure 2.** DS NPCs adopt a more glial-predominant progenitor phenotype. Fluorescent photomicrographs show vimentin and nestin immunostaining of both DS and control NPCs. Increased expression of nestin (neuroepithelial precursor,) is seen in the control NPCs, while DS NPCs show slightly greater expression of the vimentin (radial glia). DS NPCs also show diminished levels of staining for the neuronal marker MAP2. Conversely, the DS NPCs exhibit increased expression of various glial-associated markers including CNPase (oligodendrocytes), O4 sulfatide (oligodendrocyte precursor) and GFAP (astrocyte, neural precursor marker), while no significant difference is observed for NG2 expression (oligodendrocyte precursor) between DS and normal controls. The respective cell specific markers are seen under rhodamine fluorescence.The nuclei of cells are labelled with Hoechst (DAPI fluorescence) to demonstrate cell density and uniformity of the cultures.

levels in cultures or adoption of more restricted glial progenitor lineages, we compared the cell-type-specific expression profiles between the DS progenitors and previously published datasets [NCBI, Dr Clive Svendsen GSM51360-51368 lines (32)] from long-term cultured NPCs, astrocyte progenitor cells (APCs) and oligodendrocyte progenitor cells (OPCs, Supplementary Fig. S2). Longer term cultured NPCs expressed significantly increased levels of differentiated cell markers, including GFAP (GFAP), MAPT (neuronal) and OMG/MPB (oligodendrocyte), when compared with the DS NPCs. Conversely, the APC and OPC lines expressed significantly reduced levels of these mature cell markers compared with the DS NPCs. Thus, while the DS progenitors had adopted certain glial progenitor characteristics, these features did not appear to result from increased NPC maturation or adoption of astrocyte or oligodendrocyte progenitor phenotypes alone.

## Gene ontology comparison analysis

To identify functional modules of gene expression and interacting partners that were relevant to the DS gene expression signature, we applied network-based analysis through the Ingenuity Pathways Knowledge Base (IPA) (33). The initial pairwise comparisons between multiple DS and control NPC microarray profiles yielded 1902 candidate transcripts with *P*-value thresholds of $<0.05$. Of this group, only 608 candidates were shown also to have at least an absolute 1.5-fold expression change relative between the DS and control samples. Fisher's exact tests were then performed to determine the likelihood that these genes of interest participated in a given function or pathway, relative to the total number of occurrences of these genes in all functional/pathway annotations stored in the IPA. These analyses produced 334 candidate genes that could be placed into 46 networks. The top four networks incorporated 90 of the candidate genes within a network of 140 molecules with significance *P*-values between 10E-27 and 10E-37 (Fig. 3A). These networks were predicted to be involved in cell death and oxidative stress through various signaling mechanisms including the JAK/STAT canonical pathway (Fig. 3B).

Our observation that the trisomy 21 in the DS NPCs resulted in an approximate 1.5-fold increase in expression of the DS

**A**

| ID | Molecules in Network | Score | Focus Genes | Top Function |
|---|---|---|---|---|
| 1 | Akt, ***ANGPTL1, CHD4,*** Cyclin A, Cyclin E, ***DAXX,*** E2f, ***E2F3, FGF1, GCLM, GMNN, GRB10, HOXB7, HSF1,*** Hsp27, Hsp70, Hsp90, ***HSPA4, KRT10*, MCAM*,*** Mek1/2, ***MLL, MYBL2, PPP1R15A (includes EG:23645),*** Rb, ***SMARCA2*, SNRPG, SP4, SULF1*, TACC1, TAF9, TAF15, TFDP2, UXT,*** Vegf | 37 | 25 | Cell Cycle, Cellular Function and Maintenance, Gene Expression |
| 2 | ***ACTC1,*** Actin, Adenylate Cyclase, ***AQP4*,*** Calmodulin, CaMKII, Caspase, ***CDC42BPG, CITED2,*** Ck2, ***EIF4G1,*** F Actin, ***GDF15, GNAI3, GPSM2*, HADHA, HMGCS1, HTATSF1, KIAA1967, KLF15, KLHL21, MAP6, MEF2A, MYO1B, PDCD4,*** PDGF BB, ***PENK,*** PI3K, ***PNN,*** RNA polymerase II, ***SCAMP1, SNAP25, SP1, STXBP6 (includes EG:29091), WDR36*** | 37 | 25 | Cellular Function and Maintenance, Cell Signaling, Molecular Transport |
| 3 | ***ABCB4, ABCC1, ATF2,*** C1q, Cbp/p300, ***CCNB1, COL6A1,*** Creb, ***ENTPD1,*** ERK1/2, ***FKBP5, FOXM1, FTH1,*** GST, IL1, ***IRAK1,*** JINK1/2, Jnk, ***MGST1, NFE2L2,*** P38 MAPK, ***PURA*, PURB, RUNX2, SCARB1, SMAD3,*** Smad2/3, ***SOD2, SPTBN1, SSTR2,*** STAT, Tgf beta, ***TNIK, VRK1, ZFYVE9*** | 33 | 23 | Cellular Compromise, Digestive System Development and Function, Hepatic System Development and Function |
| 4 | ***APP*,*** Calcineurin protein(s), Calpain, ***CPE*, CPEB1, EPOR,*** Fgf, ***FGF12, GAP43,*** GUANYLATE CYCLASE, IKK, JAK, ***JAK1*, LIG3, LRP1,*** Mapk, Mek, ***NAGA, PICALM,*** Pka, Pkc(s), ***PKD1,*** PLC, PP2A, ***PRKCA,*** Rap1, ***S100B, SRC, STAT2*, STAT3,*** STAT5a/b, ***STAT5B,*** TCR, ***TM2D1, TUB*** | 27 | 20 | Cell Signaling, Cellular Assembly and Organization, Gene Expression |

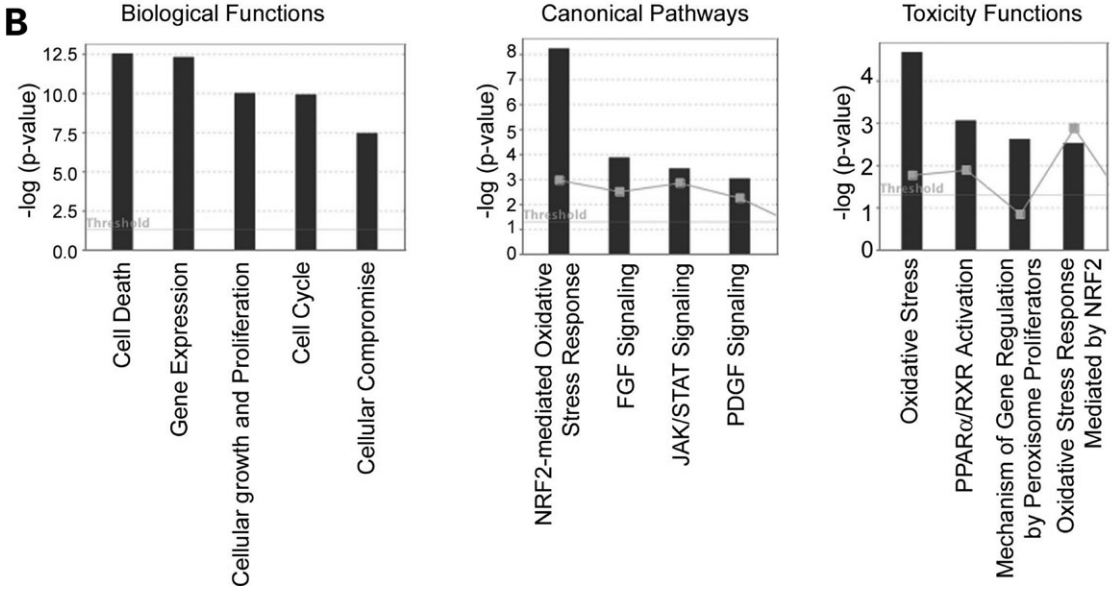


**Figure 3.** Ingenuity Pathway Analyses of differential gene expression in DS NPCs. (**A**) Interactome mapping predicts specific functional networks containing differentially expressed genes within the DS NPCs. The score reflects the statistical probability (*P*-value = 10E-27–10E-37) that the genes of interest participate in the specific pathway, relative to the total number of occurrences of these genes in all functional/pathway annotations stored in the IPA Knowledge Base. The number of focus genes indicates the number of dysregulated genes within each network of 35 genes. The top function describes the predicted function of the network. (**B**) Graphical summary of the predicted biological functions, canonical pathways and resultant toxicity expected from the differentially expressed genes.

critical region genes on microarray profiling suggested that the majority of significantly differentially expressed genes could result from downstream effects of increased gene dosage on chromosome 21. This possibility was consistent with the array data showing that relatively small 1.5–2-fold upregulation of genes on chromosome 21 resulted in a global effect on gene expression throughout the DS NPC transcriptome (Supplementary Fig. S3). Of the four networks identified by IPA analyses, the fourth network implicated two chromosome 21 genes, S100B and APP, in functional pathways that also incorporated multiple genes that were found to be dysregulated within the DS NPC gene expression profiles (Fig. 4). Both S100B and APP have previously been implicated in DS neurotoxicity from elevated expression of free radicals (34–37). Of these proteins, S100B is also found predominantly in the glial cell lineages, promotes astrocytosis and is increased in DS brain (38–42). Collectively, these findings suggested that DS NPCs harboring duplications of S100B possessed elevated levels of ROS and activated the JAK/STAT and MAPK stress response kinase pathways.

### S100B-induced oxidative stress promotes activation of stress response kinases in human DS NPCs

As a first step in investigating this potential pathway, we wanted to confirm that the profiling changes seen on comparison of the DS and control progenitors did not merely reflect differences in cell types between the experimental and control NPC lines. More specifically, S100B expression has been associated with gliogenesis, and given that the DS progenitors appeared to adopt more gliocentric progenitor phenotypes, we wanted to exclude the possibility that the increased glial pro-

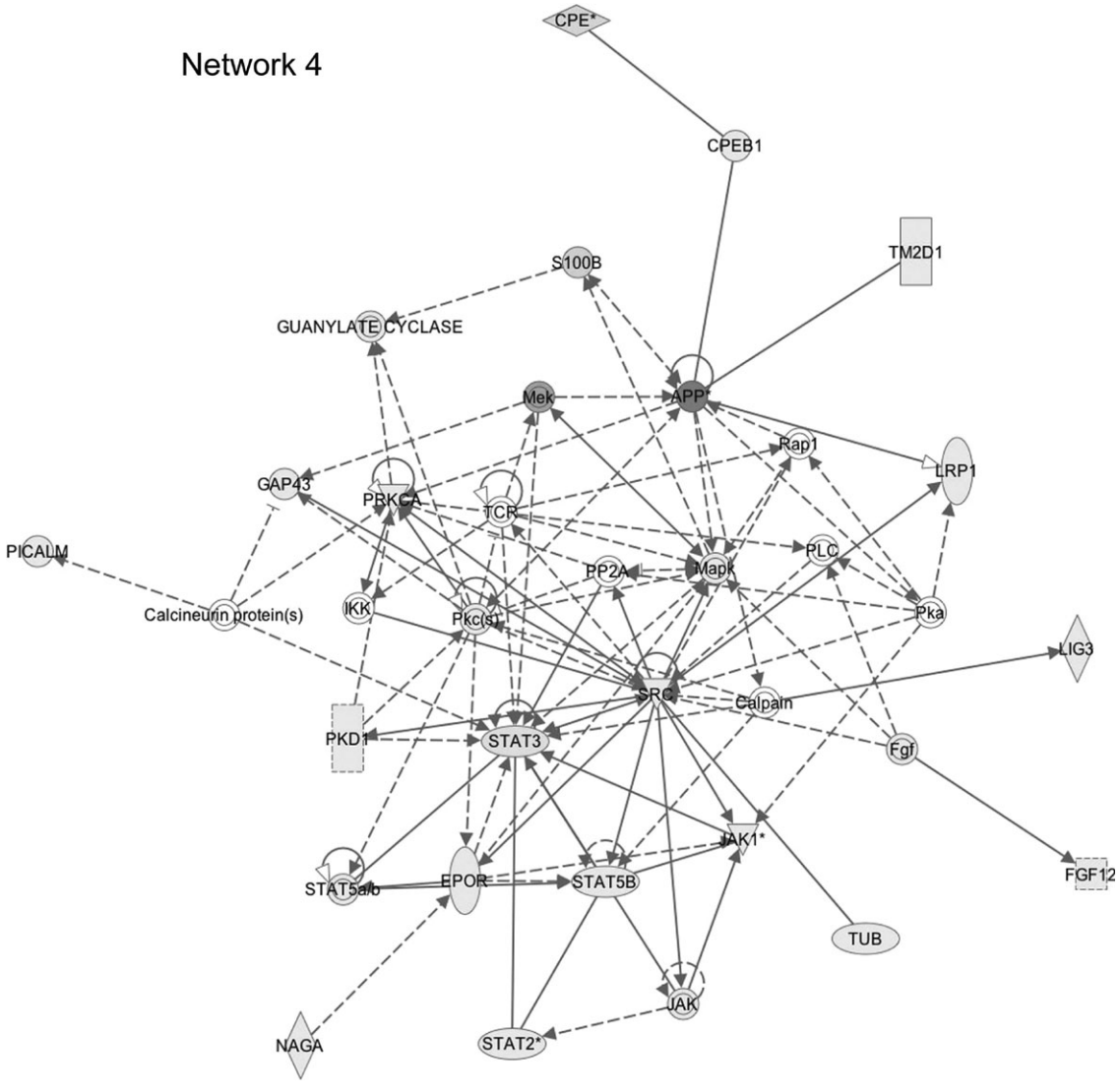


**Figure 4.** Schematic of network #4 demonstrates that many of the differentially expressed genes in the DS NPCs form tight interrelationships within known pathways involved in cell signalling, cell assembly and organization and gene expression. Multiple upregulated genes (darker shapes) form known interactions with each other suggesting a striking robustness of altered gene expression in DS NPCs. Constitutively overexpressed genes on chromosome 21 (S100B and APP) are predicted to alter STAT/JAK and MAPK activity.

genitor phenotype was responsible for differences seen in expression levels for these genes within the IPA predicted network. Expression profiling of long-term cultured NPCs showed markedly increased expression of GFAP, MBP and OMG compared with the DS progenitors. Despite this increase in glial marker levels, expression of genes within the pathway (i.e. S100B, APP, STAT2/5) was still disproportionately greater in the DS NPCs, indicating that cell type specificity alone was not responsible for differential gene expression (Supplementary Fig. S2). Similarly, the upregulation of these specific genes within the DS NPC network was not appreciated within the expression profiles for the APC or OPC cell lines.

As the microarray and network analyses provided a platform to identify potential pathways important for DS, we next sought to examine whether these processes could be appreciated functionally on a cellular level. Increased oxidative stressors and free radical scavenging have previously been reported in differentiated DS neurons and genes involved in these same pathways were apparent in DS NPCs by microarray profiling (19,20,43). We therefore asked whether hydrogen peroxide ($H_2O_2$) generation and malondialdehyde (MDA) formation, markers of ROS formation and cell lipid membrane peroxidation products, respectively, were actually altered in DS neural progenitors. Prior to and up to 48 h after induction of differentiation, both $H_2O_2$ and MDA levels increased to a greater degree and in a parallel and time-dependent fashion within DS as opposed to control neural precursor cells (Fig. 5A and B). Moreover, S100B was increased in the DS NPCs and stimulation of the DS progenitors with S100B led to further increases in oxidative stress generation after 24 h. This response was mitigated by pre-incubation with the specific S100B neutralizing antibody, antibodies to the S100B RAGE receptor, or free radical scavengers, tocopherol and ascorbic acid.

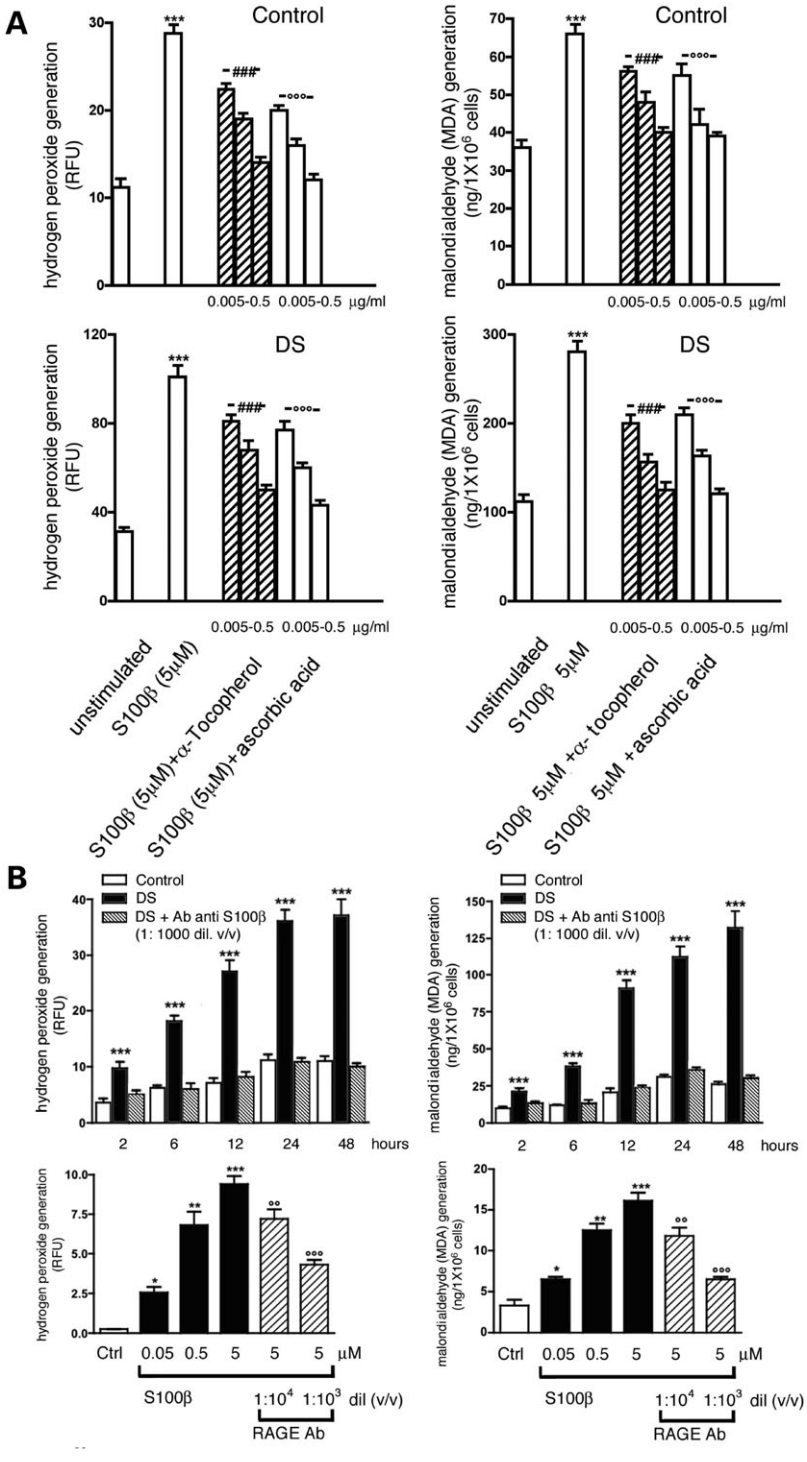


**Figure 5.** Increased free radicals and lipid peroxidation by-products in human DS NPCs. (**A**) Levels of hydrogen peroxide ($H_2O_2$) and malondialdehyde (MDA, marker of lipid peroxidation) are increased in unstimulated DS NPCs compared with control. Stimulation of both control and DS NPCs by S100B, a calcium/zinc-binding protein implicated in the activation of ROS generation, leads to further increases in free radical and lipid peroxidation by-products. S100B-induced generation of ROS can be inhibited by free radical scavengers, alpha-tocopherol and ascorbic acid in a dose-dependent fashion ($^{***}P < 0.001$ compared with unstimulated; $^{\#\#\#}P < 0.001$ and $^{ooo}P < 0.001$ compared with 5 μM S100B stimulus). (**B**) Free radicals and lipid peroxidation by-products also increase following induction of neural differentiation in DS progenitors. Both control and DS progenitors gradually accumulate increasing levels of intracellular $H_2O_2$ and lipid peroxidation by-products (MDA) following withdrawal of growth factors and maintenance in serum-containing media. DS progenitors, however, exhibit much greater increases in $H_2O_2$ and MDA compared with the control cells. A significant proportion of the increase in free radicals and lipid peroxidate by-products can be mitigated by incubation of cultures with antibody to S100B ($^{***}P < 0.001$). Generation of reactive oxygen species (ROS) is also dependent on S100B activation through its RAGE receptor (receptor for advanced glycation end products). Treatment of control progenitors with S100B leads to a rise in both free radical production and lipid peroxidation, which can be inhibited by RAGE blockade in a dose-dependent fashion (1:10 000 or 1:1000 dilution). ($^{*}P < 0.05$, $^{**}P < 0.01$ and $^{***}P < 0.001$ compared with control; $^{oo}P < 0.01$ and $^{ooo}P < 0.001$ compared to 5 μM S100B stimulus in absence of RAGE Ab.).

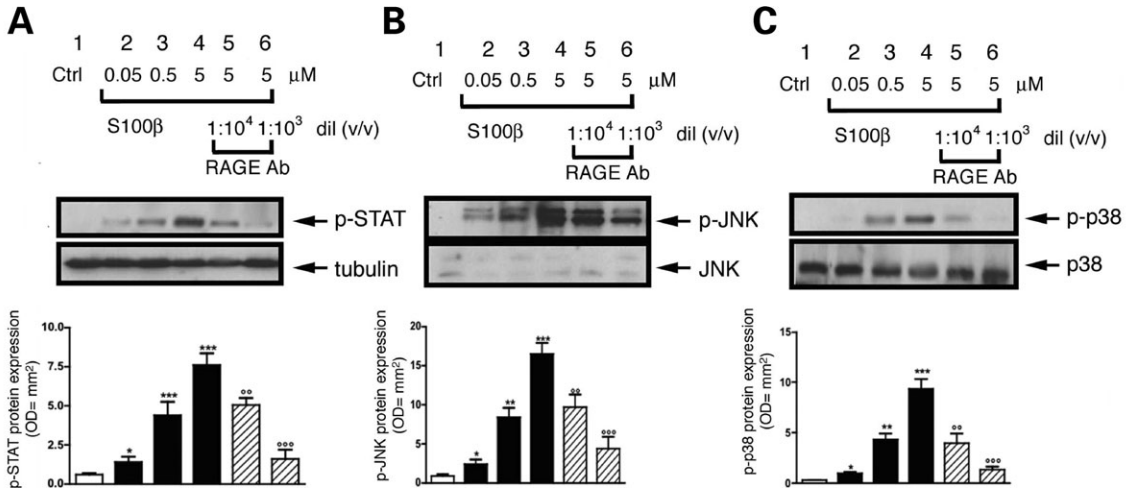


**Figure 6.** Activation of the stress activated protein kinases through S100B–RAGE interaction. S100B incubation of control progenitors leads to the phosphorylation of p38 (**A**), JNK (**B**) and STAT (**C**) pathways. Blocking of S100B with the RAGE receptor antibody inhibits activation of these stress response pathways. As S100B leads to ROS generation and increases in ROS have previously been shown to activate p38 MAP kinase and JAK/STAT phosphorylation, constitutive overexpression of S100B in DS NPCs likely promotes free radical production and stress activated protein kinase activation. ($^{*}P < 0.05$; $^{**}P < 0.01$; $^{***}P < 0.001$ compared with control; $^{oo}P < 0.01$ and $^{ooo}P < 0.001$ compared with 5 μM S100B stimulus in absence of RAGE Ab).

Both STAT/JAK and MAP kinase pathways take part in response to stress stimuli, such as cytokines, free radical injury and osmotic shock (44,45). In this respect, the findings of S100B-induced oxidative stress within DS NPCs could lead to activation of these kinase pathways, as predicted by the network analyses. To address whether S100B exposure could induce activation of these stress activated protein kinases, control NPCs were pre-incubated in S100B and phosphorylation states of the proteins were evaluated by western blot analyses. We observed a dose-dependent increase in the expression levels of the activated forms of both the MAP (p38MAP and JNK) and STAT kinases after incubation in S100B for 1 h. Furthermore, pre-incubation with the neutralizing antibody for RAGE before S100B exposure significantly inhibited S100B-induced p38MAP kinase, JNK and STAT phosphorylation in a dose-dependent manner (Fig. 6). Finally, both SB203580 and SP600125, specific and selective inhibitors of p38 and JNK respectively, inhibited S100B-induced expression of these proteins (data not shown). Given the constitutive increase in S100B from the duplication of chromosome 21 in DS, these findings suggested that overexpression of S100B likely induces ROS generation and consequent activation of MAPk and STAT/JAK pathways.

### Downstream induction of AQP4 in response to S100B overexpression in DS NPCs

Oxidative stresses and stress response kinase activation are known to alter cell proliferation, differentiation and apoptosis (44,45). Each of these developmental functions should be reflected in downstream activation of non-chromosome 21 genes in the DS NPCs. In evaluating the other highly scored, predicted IPA networks (#1–3, Fig. 3A), the top functions of these pathways were involved cell cycle (proliferation), cellular function and maintenance (differentiation and survival) and cellular compromise (apoptosis). Because the S100B and APP have both been implicated in cell toxicity from free radical generation, we focused on the second and third networks. Network #3 already shared significant overlapping interactors with network #4 (including the JAK/STAT and p38 MAPK molecules). Network #2 could similarly be linked to network #4 (Supplementary Fig. S4), but several observations also suggested that proteins in this functional pathway might serve a compensatory role in DS. Among the 25 focus genes that were differentially expressed in the array profiling for this network, several genes have previously demonstrated functions in the inhibition of inflammatory cytokines (GDF15), promoting cytokine degradation (EIF4G1), as well as regulation of hypoxia inducible factors (CITED2) and maintenance of water homeostasis (AQP4). As stress kinase activation has been associated with cytokine, ROS and osmotic changes, activation of these genes would be consistent with a secondary response to S100B induction of STAT/JAK and p38MAPK.

Several additional observations reinforced a potential link between S100B and AQP4 in DS during brain development. Both S100B and AQP4 proteins are found predominantly in glial cell lineages, associated with elevated levels of ROS and increased in various neuropathological conditions involving cell injury and death (38–40). Recent studies have also shown a concomitant increase in S100B and AQP4 after traumatic spinal cord by microarray profiling (46,47). To further explore this predicted relationship, we first confirmed the increase in AQP4 expression seen on profiling of the DS NPCs. The mRNA transcripts for AQP4 demonstrated upwards of a 3-fold increase compared with controls on multiple probe sets ($P < 0.0002$ on pairwise comparison). An increase in both the AQ4 mRNA and protein levels was also seen in the DS NPCs as well as the human and mouse DS brain tissues, further confirming upregulation of this water channel in response to duplication of some subset of gene(s) on human chromosome 21 (Supplementary Fig. S5). Second, we addressed whether the increase in chromosome 21-located S100B following induction of differentiation

within DS progenitors led to a consequent increase in expression for the chromosome 18-located AQP4. Within DS neural progenitors, a time-dependent and parallel increase in AQP4 and S100B expression was seen up to 48 h after induction of differentiation (Fig. 7A). Moreover, pre-incubation with S100B neutralizing antibody almost completely abolished the time-dependent increase in AQP4 protein, suggesting a causal relationship independent of neural differentiation. Third, we asked whether S100B and/or ROS exposure could similarly promote AQP4 expression within control neural progenitors. By 24 h after S100B (0.05–5 μM) stimulation, both AQP4 transcription and protein expression was increased in a dose-dependent fashion (Fig. 7B). Concurrently, neutralization of the S100B receptor by pre-incubation with RAGE antibody significantly inhibited S100B-induced AQP4 mRNA and protein upregulation. A similar induction of AQP4 expression was achieved by direct stimulation of progenitors with $H_2O_2$. Finally, the introduction of free radical scavengers could mitigate the S100B-induced expression of AQP4 in both control and DS NPCs (Supplementary Fig. S6). Collectively, these results suggested that constitutive overexpression of S100B in DS progenitors led to increased intracellular ROS and stress activated kinase activation, followed by the induction of AQP4 water channels.

### AQP4 mitigates S100B-induced programmed cell death through clearance of ROS

While the IPA networks and cellular studies demonstrated interactions between S100B, the stress activated kinases and AQP4, we wanted to understand the functional consequences of these gene changes. Prior work had indicated that aquaporin water channels might maintain water homeostasis by facilitating clearance of water from the extravascular space and also served to transfer intracellular ROS to the extracellular space (38,39,48). As our observations suggested a role for these genes in oxidative stress, we asked whether AQP4 could serve as a compensatory response to the S100B-induced elevation in ROS seen in the DS NPCs. We measured changes in free radicals levels caused by S100B after inhibiting AQP4 water channel expression. AQP4 mRNA transcripts and protein expression were inhibited by siRNA within human SHSY5Y neuroblastoma cells (Fig. 8) (49). Human SHSY5Y neuroblastoma cells were used given their high transfection efficiency. Decreased AQP4 mRNA levels were appreciated by 24 h with a significant inhibition of AQP4 protein levels apparent by 48 h. Loss of AQP4 function resulted in a dramatic increase in free radicals (ROS and lipid peroxidation by-products) following S100B exposure, suggesting that these water channels reduce buildup of intracellular ROS levels within neural cells.

As increases in free radicals within progenitors cause apoptosis (Supplementary Fig. S6), an upregulation in AQP4 could serve to mitigate the effects of these free radicals and provide a protective mechanism against cell death. To address this possibility, we initially examined whether S100B application to NPCs promoted caspase3 activity (a mediator of apoptosis), as predicted in the network analyses (Supplementary Fig. S4). Treatment of NPCs with 5 μM S100B-induced cleavage of pro-caspase into active caspase3 and promoted cell death, as evidence by trypan blue incorporation (Fig. 9). As expected, inhibition of AQP4 through RNA interference led to an increase in both caspase3 activation and cell death within SHSY5Y neuroblastoma cells.

## DISCUSSION

Several observations arise from the current studies examining the cellular and molecular characteristics of human DS neural progenitors. First, genetic profiling of the human DS NPCs suggest that these cell lines retain progenitor properties, differ significantly from age-matched control NPCs and adopt a more gliocentric progenitor phenotype. Second, gene ontology comparison analyses further show that networks of interacting, differentially expressed genes in the DS progenitor were associated with cell cycle (proliferation), cell function and maintenance (differentiation and survival) and cellular compromise (cell death). Moreover, some of these genes were implicated in oxidative stress toxicity and JAK/STAT canonical signaling. Third, significant but specific changes in gene transcriptional levels were seen throughout the genome, indicating that primary changes in gene expression on chromosome 21 lead to secondary, potentially compensatory changes on non-chromosome 21 genes. For example, the chromosome 21 located S100B could induce ROS generation, stress response kinase activation and upregulation of chromosome 18 located AQP4 water channel expression. While S100B promoted cell death through ROS generation, AQP4 overexpression led to a reduction in intracellular ROS and overall cell death. More broadly, these studies provide some of the first evidence that NPCs derived from a human disorder can be used to explore disrupted cellular and molecular mechanisms that give rise to a disease phenotype.

### Distinct functional pathways in DS NPCs

DS NPCs differ from WT control NPCs. Microarray profiling suggests that the DS progenitors across several different individuals appear fairly uniform in their gene expression patterns, but significantly differ on comparison to normal, age-matched controls. Network analysis further implicates several expected pathways involving gene expression, cellular growth and proliferation and cell death/compromise. Given duplication of chromosome 21, DS progenitors might be expected to show increased expression of genes involved in transcription and translation (50). While the DS NPCs maintain core expression of genes associated with self-renewing progenitors, they more surprisingly share features typically seen in glial progenitors and upregulate genes involved in cell proliferation. The gliocentric features may in part arise from a self-selection process, whereby neuronal progenitors are more susceptible to cell death or impaired development (35). The similar gene expression patterns seen across multiple DS as compared to control NPC lines and the identical culturing conditions, however, would also argue that intrinsic activation of genetic pathways in the DS cells are likely responsible for these changes. In retrospect, induction of glial and cell growth networks might even be expected as cell injury and death through ROS can promote cytokine release (such as

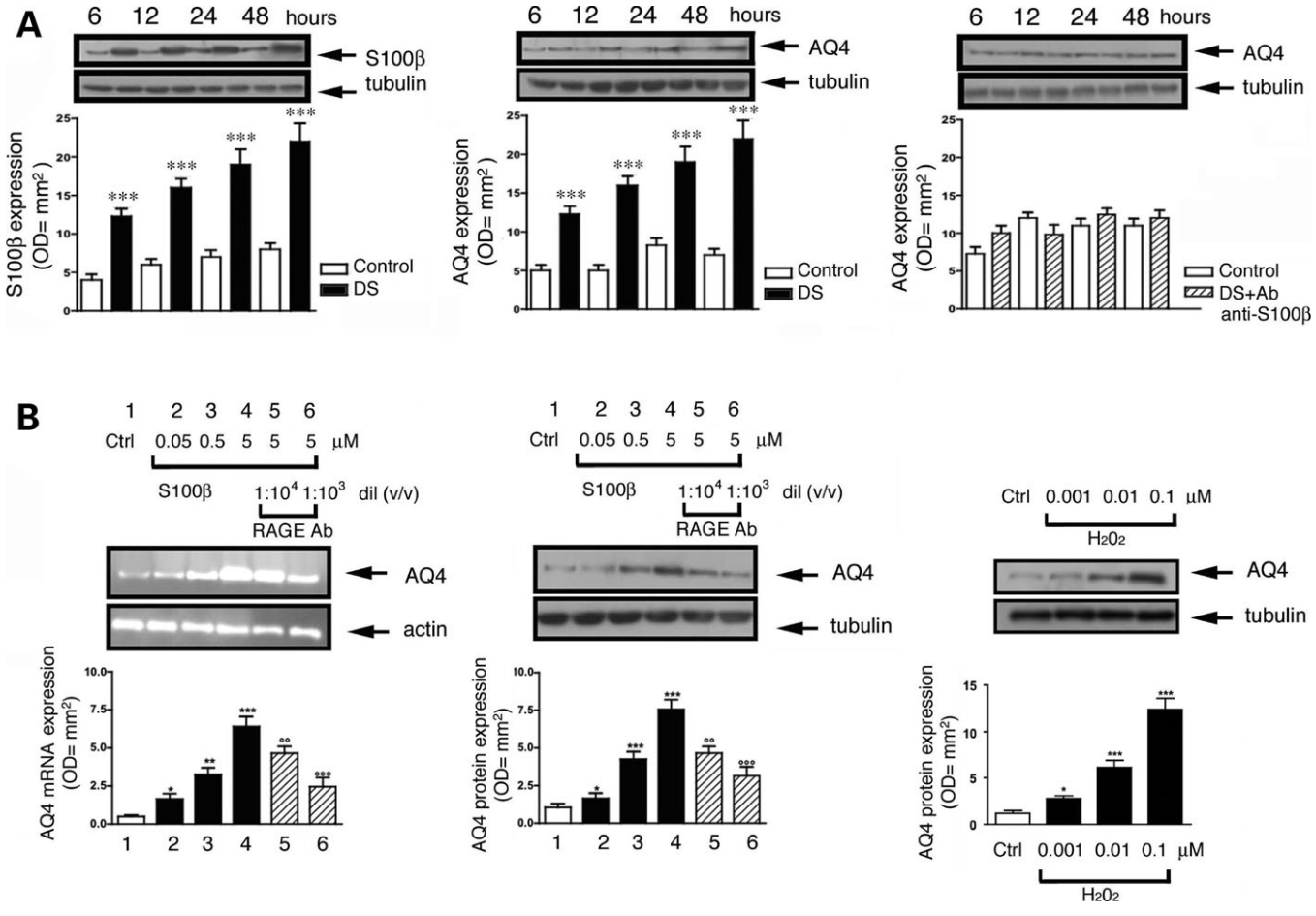


**Figure 7.** S100B induction of AQP4 expression in neural progenitors. (**A**) Increased S100B protein expression in DS versus control neural progenitors is seen following induction of neural differentiation and protein extraction for western blot analyses. Neural differentiation is induced by withdrawal of EGF and FGF and culturing of neural progenitors in serum-containing media. Increases in AQP4 expression can also be inhibited by the addition of soluble antibody to S100B to the culture media, suggesting a causal relationship (***$P < 0.001$ versus control NPC at same time point). (**B**) S100B through its RAGE receptor can promote transcriptional and translational induction of AQP4 through ROS generation. S100B treatment of control human progenitors induces AQP4 expression at both the mRNA (left, by RT–PCR) and protein (middle by western blot) levels. Blocking of the RAGE receptors (1:10 000 and 1:1000 dilution vol/vol of RAGE antibody) leads to a reduction in AQP4 expression. Direct application of $H_2O_2$ onto neural progenitor cultures leads to a dose-dependent increase in AQP4 expression (right) and free radical scavengers can block S100B-induced expression of AQP4 (Supplementary Fig. S10), suggesting that increased free radicals due to constitutively overexpressed S100B in the DS neural progenitors contributes to the increase in AQP4 levels. (*$P < 0.05$; **$P < 0.01$ and ***$P < 0.001$ compared with control; °°$P < 0.01$ and °°°$P < 0.001$ compared with 5 μM S100B stimulus in absence of RAGE Ab.).

EGF, FGF) and consequent proliferation and astrocytosis (51,52). Further investigation of the cellular and molecular mechanisms underlying these differences in progenitor characteristics, however, clearly will be necessary to understand these processes. Finally, while inflammation and neurodegeneration are often invoked in the later onset AD seen in DS, the current findings would suggest that ongoing cell injury and damage already can be appreciated early in development. The upregulated expression of genes involved in oxidative stress and cell death (network #4) provides a partial mechanistic basis for the DS phenotype.

## Genome-wide dysregulation of gene expression in DS NPCs

While primary gene dosage effects have been shown in various DS tissue (53), the nature and extent of trisomy 21 in effecting secondary disomic genes is unclear. Some studies have suggested that while changes in transcript levels occur in the trisomic genes, no pervasive effect is seen on gene expression on chromosomes other than 21 (54–56). Alternatively, other work has argued that overexpression of trisomy 21 can lead to profound disruption of the entire transcriptome (57–59). The present study suggests that trisomic genes do lead to specific changes in transcript expression on each of the non-chromosome 21 genes (so termed, global dysregulation), but only in fairly specific pathways. Of the ~50 000 transcripts, only 1900 transcripts (3.8%) were found to be significantly different on pairwise comparison of multiple control and DS samples. Moreover, of these 1900 transcripts, only 330 transcripts (0.07%) were shown to significantly interact on network analysis and the levels of abnormal expression were generally only 1.5–2-fold in excess/deficit compared with normal. Thus, our findings are compatible with both views in that we observe a global dysregulation in gene expression with increases in non-chromosome 21 genes

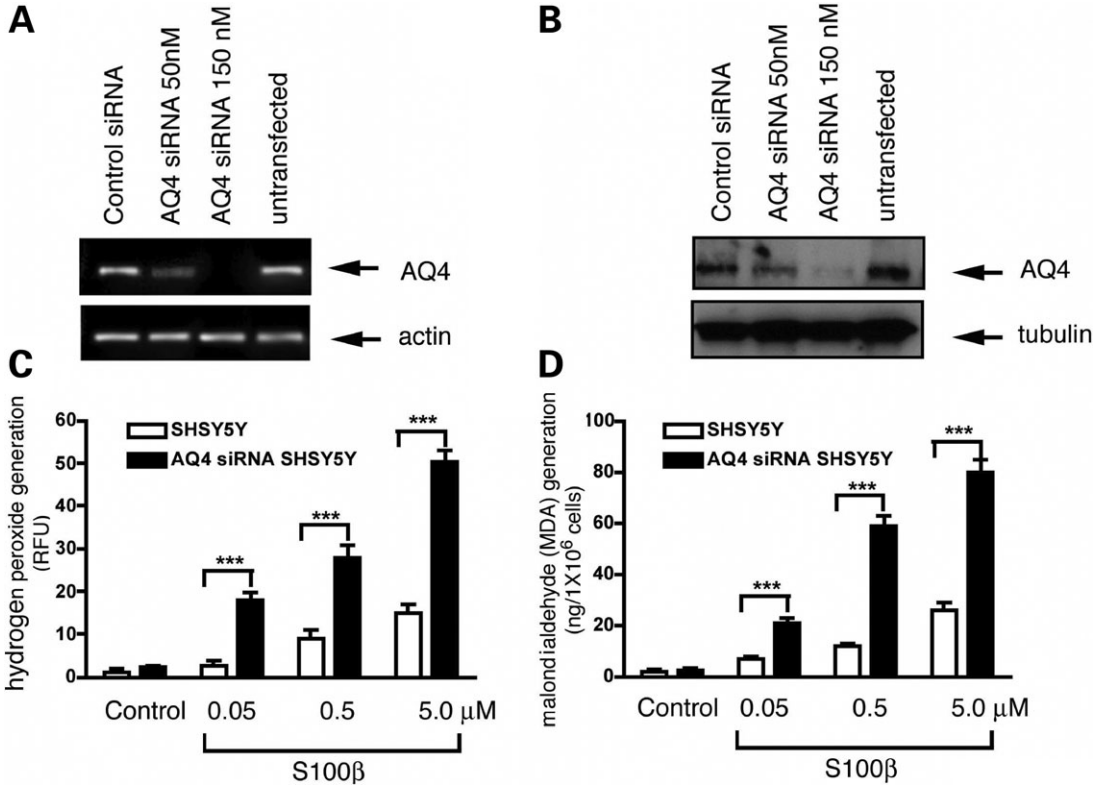


**Figure 8.** Inhibition of AQP4 expression leads to increased S100B-induced ROS levels in human SHSY5Y neuroblastoma cells. (**A**) Decreased expression levels of AQP4 mRNA can be seen by RT–PCR at 24 h following transfection of the siRNA AQP4 construct, as compared to control (Cyclophilin B siRNA) and untransfected cells. (**B**) Decreased expression levels of AQP4 protein can be seen by western blot analysis at 48 h following transfection of the siRNA AQP4 construct as compared to control (Cyclophilin B siRNA) and untransfected cells. (**C** and **D**) S100B-induced ROS ($H_2O_2$ and MDA generation) are potentiated with inhibition of AQP4 channel expression, suggesting that the water channels assist in the clearance of free radicals ($^{***}P < 0.001$).

at both the mRNA and protein levels, but find that these changes occur only in a very specific and selective subset of genes. These observations would be consistent with the interpretation that increased expression of genes on chromosome 21 within neural cells leads to specific compensatory changes in expression of genes found off of chromosome 21.

The relatively specific changes seen on the secondary non-chromosome 21 transcriptional profiling from these studies, as compared to prior reports, may extend from several factors: (1) tissue specificity, (2) modest changes seen on genes expression from DS transcriptional profiling and (3) use of cultured NPCs as opposed to tissue. First, prior studies demonstrating no clear changes in secondary transcriptional effects from DS typically used human or mouse samples, composed of mixed cell populations from whole brain, cerebellum or heart tissues (55,56). The current studies rely on temporal, regional and cellular specificity for mRNA profiling. NPCs were generated from a fairly narrow window in human cortical development (gestational ages 19–21 weeks), isolated from a specific area of the ventricular zone along the frontal cortex, and expanded by EGF and FGF to generate primary neural progenitors. In this manner, the secondary changes seen in non-chromosome 21 genes for the current studies may reflect specific differences for a particular cell population in the brain during development. Second, we also find that 1.5–2-fold difference changes in chromosome 21 gene expression result in only modest fold changes in expression of non-chromosome 21 genes. These findings are similar to those by FitzPatrick *et al*. (57) who used DS amniocyte cultures and found only modest changes in the average level of transcription. Presumably, the whole tissue containing mixed cellular populations used in some prior studies might mask these more subtle findings, given the complexity of gene expression for different cell types. Finally, transcriptional profiling for these experiments was performed on cultured NPCs. These experiments used pairwise comparisons between DS and normal NPCs, which are generated and maintained under identical conditions *in vitro*, thereby suggesting that the observed differences likely have important functional implications. Moreover, some of the observed changes do correlate with gene and protein expression in tissue such as AQP4 and S100B upregulation. However, the extent to which cell culture modifies gene transcriptional levels in DS is not known.

### S100B and AQP4 regulation of free radical mediated cell death in DS NPCs

While overexpression of such proteins as S100B and APP are thought to contribute to the neurodegenerative features of DS and AD (19,20,42), we now find that these same processes are apparent very early in neural development and within the

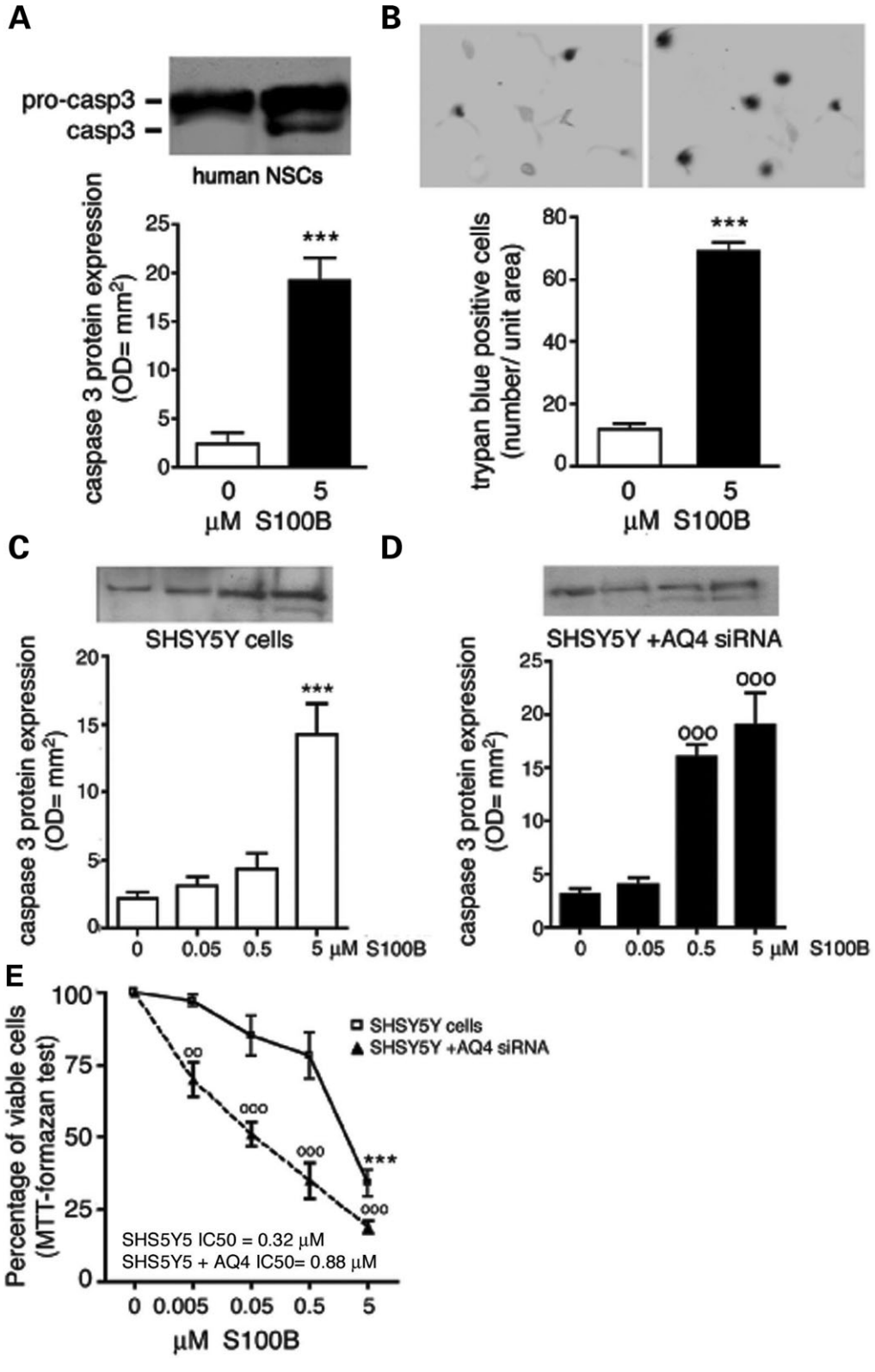


**Figure 9.** Inhibition of AQP4 expression leads to increased cell death in human SHSY5Y neuroblastoma cells. (**A**) S100B exposure results in activation of caspase3 and (**B**) increased cell death by trypan blue incorporation. Control NPCs are harvested for western blot analysis of caspase3 activity and examined in culture for trypan blue exclusion following 6 h incubation in 5 μM S100B. (**C**) S100B can induce a similar activation of caspase activity in human neuroblastoma SHSY5Y cells in a dose-dependent fashion. (**D**) S100B-induced caspase3 activity is increased with inhibition of AQP4 by RNA interference. Differences in levels of activation of this apoptotic protease following AQP4 inhibition are best appreciated following 0.5 μM S100B incubation for 6 h. (**E**) S100B-induced ROS levels and caspase activity correspond to a decline in SHSY5Y cell viability. Inhibition of AQP4 prior to S100B exposure leads to a further decline in cell viability ($^{***}P < 0.001$; $^{ooo}P < 0.001$; $^{oo}P < 0.01$ versus untreated). IC50 = minimum concentration of S100B required to achieve 50% cell viability.

neural precursor population. More specifically, the induction of ROS generation through S100B expression seen in the neural progenitors during development parallels the mechanisms of cell injury postulated for the calcium-binding protein in neurodegeneration. S100B is constitutively overexpressed in glia throughout life given its location on chromosome 21 (37,42). Activated astrocytes release the calcium-binding protein which activates the receptor for advanced glycation (RAGE), induces ROS generation and p38 MAPkinase upregulation (40,60). This presumed inflammatory process from S100B is implicated in plaque formation and neuronal degeneration in AD (36,38,61). A nearly identical response can be seen in the neural progenitors. That said, these observations may not be so surprising, given that insults from many degenerative processes are thought to be progressive and cumulative.

The increase in S100B and free radicals leads to the consequential upregulation of AQP4 water channels. Consistent with some role in water clearance and neuroprotection, increased AQP4 expression has been associated with brain swelling from strokes, head injuries, brain tumors and brain abscesses (62). AQP4 expression in glial foot processes near blood vessels, the neuroependyma (and NPCs) and pial surface has led to the paradigm that these channels serve to maintain water balance in the brain by shunting water out of the extracellular space and into the vasculature or cerebrospinal fluid (63–66). However, prior reports show that null *AQP4* mice do not develop severe brain edema following injury, raising the question of whether induction of these water channels after injury is intended for the maintenance of water homeostasis (67,68). The current network analyses suggest that AQP4 is linked to mediators of ROS and stress response kinases. Moreover, cell oxidative stressors appear to be sufficient to induce water channel expression, perhaps in promotion of cell survival. A similar transfer of intracellular ROS to the extracellular space has been proposed in plant cells (48).

### General role of NPCs derived from CNS developmental disorders in studying human disease

Several approaches have been used to study the molecular genetics and pathology of DS. Mouse aneuploidies have been used to model DS, either trisomy 16 (embryonic lethal), partial trisomy 16 (trisomy strains Ts65Dn and Tc1Cje) and most recently, a mouse containing an almost complete copy of human chromosome 21 (strain Tc1) (69,70). Chromosome 16 in the mouse contains approximately two-thirds of the homologous genes found on human chromosome 21. An alternative model is now provided by the use of human DS neural progenitors and neurons. The ability to expand and generate large numbers of human progenitors affords the opportunity to study the molecular and cellular aspects of DS. Human progenitors offer the added advantage that three complete copies of genes on human chromosome 21 including the upstream and downstream regulatory elements are replicated in each cell. The complete genetic makeup of the human cells will likely serve to enhance the validity of altered molecular pathways observed from changes in expression of genes found both on and off chromosome 21.

Previous analyses of human DS neural precursors and neurons in culture have allowed for characterization of some potential aberrant pathways in this disorder. Primary cortical neurons from gestational 16–18 week fetal DS brain fail to survive long-term in comparison to normal cultures, even in the presence of serum with survival factors, due to increased ROS, mitochondrial dysfunction and aberrant APP processing (19,20). More recent studies using DS neural progenitors showed that SCG10, a neuron-specific growth-associated protein regulated by the neuron-restrictive silencer factor REST, was almost undetectable in the DS sample, consistent with a reduction of cortical neurons in DS brain (21). However, we noted minimal expression of REST in either the DS or the control NPC population, in support of findings reported by Sohn *et al*. (71). The discrepancy may be due to different culturing techniques although the current work and the Bahn *et al*. (21) studies both rely on EGF and FGF for NPC propagation. More likely, the current work utilized progenitors derived from a later stage in fetal development, 19–22 weeks as opposed to 8–18 weeks reported in the prior work. In this respect, our findings could support the Bahn results, as an early decline in neural precursors, which have a greater capacity to generate neurons, could give rise to the neural precursors derived from the current studies, which exhibit more glial-related properties.

## CONCLUSION

DS is a complex genetic condition arising from an altered dosage of WT genes on human chromosome 21. As seen in the current study, variations in gene dosage on chromosome 21 can lead to altered gene expression on non-chromosome 21 genes. These changes outside of chromosome 21 may reflect both compensatory cyto-protective mechanisms, as well as effectors of neuropathology. In this respect, and particularly in the case of the human nervous system, the disrupted signaling cascades in human neural precursors and neurons may not necessarily be shared across other mammalian species. Isolation of hNPCs as models of human disease provides a means to functionally test and correct potential altered cellular and molecular pathways distinct for DS as well as other various disorders of the CNS.

## MATERIALS AND METHODS

### Human tissue, ethical and licensing considerations

The study has been approved by the Institutional Review Board (IRB) at the Beth Israel Deaconess Medical Center and Brigham and Women's Hospital. De-identified human discarded tissue was obtained from pathological samples during autopsy. Neural progenitors from three DS and three age-matched control brains (gestational ages 19–21 weeks) were used in this study for each of the experiments described.

### Antibodies and reagents

Antibodies used for immunostaining and western blot analyses are as follows. Anti-GFAP (1:100; DAKO, Carpinteria, CA, USA); anti-O4, anti-CNPase, anti-NG2 and anti-nestin

(1:100; Chemicon, Temecula, CA, USA); anti-vimentin and anti-MAP2 (1:100; Sigma, St. Louis, MO, USA), anti-mouse AQP4 (1:100, Novus Biologicals), anti-human AQP4 (1:1000; Acris antibodies, Hiddenhous, Germany) anti-S100B (1:250; AbCam, Cambridge, UK), p-p38MAPK(1:500; Pharmingen, Milan, Italy), anti-pJNK (1:500; Santa Cruz Biotechnology, La Jolla, CA, USA), anti-pSTAT (1:500; Santa Cruz Biotechnology) and anti-caspase3 (1:500; Sigma, Milan, Italy).

*Tissue dissociation and isolation*. Methods for ventricular zone dissection and dissociation follow general guidelines used in murine samples (72). In brief, samples were obtained along the periventricular zone within the frontal cortex (Supplementary Fig. S1A), minced and washed in cold Hank's buffered saline solution and placed in trypsin solution at 37°C for 30 min. The sample was then strained through a 40 μ cell strainer (Falcon, San Jose, CA, USA), and washed in Dulbecco's modified eagle medium (DMEM) with 10% fetal calf serum (FCS) (Hyclone, Logan, UT, USA) to inactivate the trypsin. The dissociated cells were spun down, the media aspirated and cells were placed in at low dilution ($1 \times 10^5 - 1 \times 10^6$per 5 ml) in neurosphere medium (NM, Clontech bullet kit) for expansion. The cultures were maintained in a 37°C/5% $CO_2$ incubator and media was renewed weekly. To differentiate cells and with initiation of the culture experiments, NM was replaced by DMEM with 10% FCS or neurobasal/B27 media supplemented with L-glutamine and streptomycin/penicillin (5 μM).

SHSY5Y cell cultures were maintained as follows. Cells were cultured in DMEM with 10% fetal bovine serum (FBS) for 3 days. The FBS content of the culture medium was then reduced to 5%, and the cells were exposed to 10 μM retinoic acid. The cells were kept under these conditions for 5 days, changing the medium every 2 days. Subsequently, the cells were cultured in Neurobasal/B27 medium supplemented with B-27, retinoic acid (10 μM), L-glutamine and streptomycin/penicillin (5 μM).

*Genetic analysis*. Cytogenetic analysis of the expanded DS neural precursor population was performed using standard fluorescent *in situ* hybridization techniques against chromosome 21 (73). Labeling of the BAC probes followed standard procedures with dUTP containing rhodamine and fluoroscein tags (methods outlined in the Vysis nick translation kit, Grove, IL, USA). Hybridization was performed by denaturing the slides in 70% formamide/2 × SSC, dehydrating the slides with serial ethanol washes and applying the probe to the slide samples. Post-hybridization, the slides were washed, coverslipped and examined under fluorescence microscopy (Zeiss Axioskop). Analysis of each of the progenitor lines was performed to exclude potential mosaicism in the samples.

*Microarray analyses*. Methods for Affymetrix gene chip profiling followed previously published work on gene expression in human NPCs (74). Microarray analysis was performed by Expression Analysis (Affymetrix® Genomic Processing Facility in Durham, NC, USA) using the Affymetrix HU 133 plus 2.0 chip. Total RNA (10 μg) was extracted from the neural precursors, and labeled. The target of labeled cRNA was hybridized to the GeneChip, expression values were calculated based on the difference of the perfect match oligos and mismatch in the probe set, the signal values from each array was normalized and a data file generated. Data sets were analyzed by a pairwise comparison and the Wilcoxon's signed-rank test to derive biologically meaningful results.

To ensure reproducibility and biological significance, RNA samples were collected from three DS (gestational age 19–21 weeks) and age-matched control neural progenitor lines (biological replicates). Samples were obtained within 12 h postmortem (in collaboration with the Boston hospitals and in collaboration with Drs Folkerth and Hecht). Data from microarrays were normalized using two independent methods with Rosetta Resolver software. Statistical significance of gene expression differences between neuronal subtypes was determined by pairwise comparisons at each age using Significance Analysis of Microarrays (75). Microarray data from the biological replicates were combined in Rosetta Resolver for trend plots.

For comparison studies against early and late control NPCs, APCs and OPCs, data sets from publicly available domains were used [NCBI, GSM51360-51368 from Dr Clive Svendesen and Shin and Chesnut (32)]. Relative ratios of the expression levels for genes in network #4 (APP, CPE, EPOR, FGF12, GAP43, LIG3, LRP1, JAK1, NAGA, PICALM, PKD1, PRKCA, S100B, SRC, STAT2, STAT5B, TM2D1, TUB), cell specific markers (GFAP, MBP, MAPT, DCX, OMG) and AQP4 were calculated for the respective NPC lines. Each of the datasets contained early NPC array profiling, allowing for calculation of relative rates or increase/decrease on comparison of DS versus early control, 53 week NPC versus early 15 week control and APC/OPC versus early control. The genes evaluated in network #4 represented the subset of genes that were found in common across each of the different array platforms.

*Identification of significant pathways in biological processes and altered interactome of DS NPCs genes*. The IPA is a curated database of previously published findings on mammalian biology from the public literature (Ingenuity Systems). Reports on individual studies of genes in human, mouse or rat were first identified from peer-reviewed publications, and findings were then encoded into an ontology by content and modeling experts. Manual extraction and curation probably results in more specific and comprehensive interactions, with far fewer false-positives than automated alternatives. The following steps were used (1): Genes identified as significant from the experimental data sets were overlaid onto the interactome. Focus genes were identified as the subset having direct interaction(s) with other genes in the database (2). The specificity of connections for each focus gene was calculated by the percentage of its connections to other significant genes. The initiation and growth of pathways proceeded from genes with the highest specificity of connections. Each pathway had a maximum of 40 genes (3). Pathways of highly interconnected genes were identified by statistical likelihood using equations as previously described. The IPA database was used according to the company instructions (www.ingenuity.com).

*Real time-PCR protocol*. The RT–PCR protocol followed previously described methods (76). The cDNA templates were reverse-transcribed *in vitro* (Invitrogen) using total RNA

extracted from human DS and control neural progenitors. Primers for AQP4 were designed to amplify a 200–300 bp PCR fragment. The human GAPDH gene was used as a control to normalize the amount of the paired of cDNA templates (for example, cDNA templates from control and DS neural progenitors). The PCR reaction containing SYBR Green I dye was performed in a 96-well plate using the SYBR Green Master Mix kit (Applied Biosystem, Foster City, CA, USA). PCR reaction for each cDNA sample was duplicated to reduce the chance of contamination. GAPDH was used as a control for every sample. The fluorescent intensity of PCR products was measured and quantified as numbers of amplification cycles by the ABI Prism 7700 Sequence Detection System (Applied Biosystem). The difference of PCR cycles between two cDNA samples for a tested gene was then calculated into a ratio according to the method suggested by the ABI Prism 7700 Sequence Detection System.

*ELISA protocol*. In brief, 96-well plates (Nunc 80040LE 0903) were coated with AQP4 mouse-Ab (1:300; Acris, SM1811P, Germany) (50 μl each well) at 4°C overnight, washed with PBS and blocked with 3% bovine serum albumin for 2 h at room temperature (RT). The wells were washed with PBS, samples were added (protein extracts from control and DS NPCs) and the plates were incubated for 2 h at RT. The plate was washed with PBS five times and incubated with AQP4 Rabbit-Ab (1:300; Chemicon, AB3068) (50 μl each well) for 2 h at RT. Following another PBS wash, the wells were incubated with biotinylated anti-Rabbit Ab (1:300) for 2 h at RT; washed with PBS and incubated with streptavidin-HRP from ABC kits (1:50; Vector, Burlingame, CA, USA) for 2 h at RT. The wells were then washed with PBS and incubated with ABTS (Roche Diagnostics, Indianapolis, IN, USA, 1204521) substrate for 20 min at RT. The colorimetric change in each well was measured as a change in the optical density (OD) value with an ELISA plate reader at 405/490 nm.

*Immunocytochemistry*. The neural precursors were plated onto glass slide chambers coated with poly-D-lysine (Beckton Dickenson, San Jose, CA, USA) for several hours and fixed with 4% paraformaldehyde in phosphate-buffered saline (PBS) or −80°C methanol. The cultures were placed in blocking solution with PBS containing 10% FCS, 5% horse serum and 5% goat serum or 10% donkey serum (Hyclone), incubated overnight in the appropriate antibody (Acris, aquaporin 4) and processed through standard fluorescent secondary antibodies (CY3, Jackson Immunoresearch Laboratories and FITC, Sigma).

## Measurement of ROS formation

The measurement of intracellular $H_2O_2$ was used as a marker of ROS formation. $H_2O_2$ production was evaluated by the 2′,7′-dichlorofluorescein (DCF) method according to previously described methods (40). DS and euploid NPCs, cultured in DMEM with FCS to induce differentiation, were harvested at various time points (2–48 h) after introduction of the differentiating media. Cells were detached from Petri dishes and seeded at a density of $5 \times 10^3$ cells/well into 96-well plates. 2′,7′-Dichlorofluorescein-diacetate (ICN Biochemicals, Costa Mesa, CA, USA) was then added directly to the medium at a final concentration of 5 μM and the cells were then incubated for 1 h at 37°C. H2DCF-DA is a non-fluorescent permeable molecule which diffuses passively into cells; the acetates are then cleaved by intracellular esterases to form H2DCF which is thereby trapped within the cell. In the presence of intracellular $H_2O_2$, H2DCF is rapidly oxidized to the highly fluorescent DCF.

In further experiments, euploid neural precursor cells were cultured, seeded as described above and treated with exogenous S100B (0.05–5 μM) for 0.5 h in the presence or absence of specific blocking RAGE neutralizing antibody (1:1000–1:10 000 dil. v/v; R&D Systems, Minneapolis, MN, USA). After treatment, cells were washed twice with PBS and the plates placed in a fluorescent microplate reader (LS 55 Luminescence Spectrometer, Perkin Elmer, Beaconsfield, Bucks, UK). Fluorescence was monitored using an excitation wavelength of 490 nm and an emission wavelength of 520 nm. Results were expressed as relative fluorescence units.

## Lipid peroxidation assay

Measurements of cell membrane lipid peroxidation were performed using the thiobarbituric acid (TBA, Sigma) colorimetric assay, which detects the most abundant lipid peroxidation product MDA. Methods have been described previously (77). DS and euploid neural precursor cells, cultured for different time points (2–48 h) after induction of differentiation, were washed three times with 1× PBS and then detrached from the Petri dishes by scraping in 4°C PBS. In further experiments, euploid neural precursor cells were cultured and treated with exogenous S100B (0.05–5 μM) for 1 h in the presence or absence of specific RAGE neutralizing antibody (1:1000–1:10 000 dil. v/v). Cells were then washed and detached as described above. In both experiments, cells were lysed by six cycles of freezing and thawing. One ml 10% (w/v) trichloroacetic acid (Sigma) was added to each 450 μl of cellular lysate. After centrifugation at 1000*g* for 10 min, 1.3 ml 0.5% (w/v) TBA was added and the mixture was heated at 100°C for 20 min. After cooling, MDA formation was recorded (Absorbance 530 nm and Absorbance 550 nm) in a Perkin Elmer (Massachusetts, MA, USA) spectrofluorimeter and the results are presented as ng MDA/$1 \times 10^6$ cells.

## Protein isolation and western blot analysis

Following the different experimental conditions described earlier, precursor cells ($1 \times 10^6$) were washed twice with ice-cold PBS and centrifuged at 180*g* for 10 min at 4°C. The cell pellet was resuspended in 100 μl of ice-cold hypotonic lysis buffer (10 mM HEPES, 1.5 mM $MgCl_2$, 10 mM KCl, 0.5 mM phenylmethylsulphonylfluoride, 1.5 μg/ml soybean trypsin inhibitor, 7 μg/ml pepstatin A, 5 μg/ml leupeptin, 0.1 mM benzamidine, 0.5 mM DTT) and incubated on ice for 15 min. The cells were lysed by rapid passage (5–6 times) through a syringe needle and the samples was centrifuged for 1 min at 13 000*g* for 1 min. Protein concentration was determined and equivalent amounts (100 μg) of each sample was run by electrophoresis on a 12% discontinuous polyacrylamide gel. The proteins were transferred onto nitro-cellulose

membranes, according to the manufacturer's instructions (Bio-Rad, Hercules, CA, USA). The membranes were saturated by incubation at 4°C overnight with 10% non-fat dry milk in PBS and then incubated with the antibody specified. The membranes were washed three times with 1% Triton 100-X in PBS and then incubated with anti-rabbit immunoglobulins coupled to peroxidase (1:1000; DAKO, Golstrup, Denmark). The immunocomplexes were visualized by the ECL chemiluminescence method (Amersham, Piscataway, NJ, USA). Subsequently, the relative expression of tau protein in cytosolic fraction was quantified by densitometric scanning of the X-ray films with a GS 700 Imaging Densitometer (Bio-Rad) and a computer program (Molecular Analyst, IBM).

### Cell death studies

Cell viability was measured in NPC and DS cells using the MTT (3-[4,5-dimethyltiazol-2yl]-2,5 diphenyltetrazolium bromide) assay according to the techniques described by Mosman *et al*. (78). In brief, cells were plated at the density of $1 \times 10^5$ cells/well in 96 well plates, treated with S100B (0.005–5 μM), $H_20_2$ (0.001–1 μM), or staurosporine (1–625 nM; ICN) for 24 h. After 24 h, 25 μl of MTT (5 mg/ml in DMEM/Neurobasal 1:1) was added to each well and cells were incubated for an additional 3 h at 37°C. After this interval of time, cells were lysed and dark blue crystals solubilized with 125 μl of a solution containing 50% (v/v) *N*,*N*′-dimethyl formamide, 20% (w/v) sodium dodecylsulfate with an adjusted pH of 4.5. The OD of each well was measured with a microplate spectrophotometer (Titertek Multiskan MCC/340) equipped with a 620 nm filter. Cell viability was thus calculated as % of cell viability = (OD treated/OD control) × 100.

### RNA isolation and reverse transcriptase-PCR analysis

The mRNA level of AQP4 protein in euploid neural precursor cells was determined using the semiquantitative RT–PCR method (Invitrogen, Milan, Italy). Total mRNA was extracted from cells by use of an ultrapure TRIzol reagent (Gibco BRL, Carlsbad, CA, USA) as directed by the manufacturer. The concentration and purity of total RNA were determined from the A260/A280 ratio using a UV spectrophotometer (DU 40, Beckman). The primers sequences used for PCR amplification were sense 5′-TTGTGGCAACTGAAGATGGA-3′, antisense 3′-CTGCTCTTATGGGGCAATCT-5′, and sense 5′-ATGAAGATCCTGACCGCGCGT-3′, antisense: 5′-AACGCAGCTCAGTAACAGTCCG-3′, for β-actin. 1 μg of total RNA from each specimen was subjected to RT–PCR. RT–PCR was carried out using a SuperScript TM One-step RT–PCR with Platinum *Taq* Kit (Invitrogen, Carlsbad, CA, USA) in a total reaction volume of 25 μl, containing 2× reaction mix (12.5 μl), 25 μmol/l sense primer (0.5 μl), 25 μmol/l antisense primer (0.5 μl), RT–PCR platinum *Taq* mix (0.5 μl), and autoclaved distilled water. The β-actin and AQP4 PCR products were electrophoresised on 1% agarose gel and visualized by staining with ethidium bromide. The integrated density values of the bands representing amplified products were acquired and analyzed by GS 700 Imaging Densitometer (Bio-Rad) and a computer program (Molecular Analyst IBM).

### Statistical analyses

Results were expressed as the mean ± SEM of *n* experiments. Statistical analysis was determined with ANOVA and multiple comparison were performed with Bonferroni's test, with $P < 0.05$ considered significant. The cell biological experiments were done in each of three control and DS neural lines, isolated from different individuals and results were consistent.

### siRNA synthesis and transfection of siRNA duplexes procedure

RNA duplexes of 21 nucleotides specific for human AQP4 sequence were synthesized by Dharmacon Research, Inc. (Lafayette, CO, USA). The methods followed previously published procedures (49). AQP4 sense sequence was 5′-GAUCAGCAUCGCCAAGUCUUU-3′. Cyclophilin B siRNA was used as control siRNA. SHSY5Y cells were seeded the day before transfection using an appropriate medium with 10% FBS without antibiotics. Transient transfection of siRNAs was carried out using Oligofectamine (Invitrogen), using the protocol suggested by the manufacturer. Briefly, the appropriate amount of Oligofectamine was diluted 1:5 in OPTIMEM® medium (Invitrogen) and incubated at RT for 10 min. In parallel, siRNAs were diluted 1:9 in OPTIMEM medium. The two mixtures were combined and incubated for 20 min at RT for complex formation. After addition of the appropriate growth medium with 10% FCS and without antibiotics, the entire mixture was added to the cells. Specific silencing was confirmed by at least three independent western blot and RT–PCR experiments.

## SUPPLEMENTARY MATERIAL

Supplementary Material is available at HMG Online.

## ACKNOWLEDGEMENTS

We also wish to thank Dr Roger Reeves for kindly providing tissue sections from trisomy 16 mice.

*Conflict of Interest statement*: None declared.

## FUNDING

This work was supported by grants to V.L.S from the Julian and Carol Cohen and the Ellison Foundation. V.L.S. is a Beckman Young Investigator and Doris Duke Clinical Scientist Development Award recipient.

## REFERENCES

1. Renfranz, P.J., Cunningham, M.G. and McKay, R.D. (1991) Region-specific differentiation of the hippocampal stem cell line HiB5 upon implantation into the developing mammalian brain. *Cell*, **66**, 713–729.
2. Reynolds, B.A. and Weiss, S. (1992) Generation of neurons and astrocytes from isolated cells of the adult mammalian central nervous system. *Science*, **255**, 1707–1710.

3. Gage, F.H. (2000) Mammalian neural stem cells. *Science*, **287**, 1433–1438.
4. Snyder, E.Y., Deitcher, D.L., Walsh, C., Arnold-Aldea, S., Hartwieg, E.A. and Cepko, C.L. (1992) Multipotent neural cell lines can engraft and participate in development of mouse cerebellum. *Cell*, **68**, 33–51.
5. Snyder, E.Y. and Macklis, J.D. (1995) Multipotent neural progenitor or stem-like cells may be uniquely suited for therapy for some neurodegenerative conditions. *Clin. Neurosci*, **3**, 310–316.
6. Ourednik, V., Ourednik, J., Flax, J.D., Zawada, W.M., Hutt, C., Yang, C., Park, K.I., Kim, S.U., Sidman, R.L., Freed, C.R. *et al.* (2001) Segregation of human neural stem cells in the developing primate forebrain. *Science*, **293**, 1820–1824.
7. Sheen, V.L., Ferland, R.J., Harney, M., Banham, A., Brown, P., Chenn, A., Corbo, J., Hecht, J., Folkerth, R. and Walsh, C.A. (2006) Impaired proliferation and migration in human Miller Dieker neural precursors. *Ann. Neurol*, **60**, 137–144.
8. Bhattacharyya, A. and Svendsen, C.N. (2003) Human neural stem cells: a new tool for studying cortical development in Down's syndrome. *Genes Brain Behav.*, **2**, 179–186.
9. Scheffler, B., Edenhofer, F. and Brustle, O. (2006) Merging fields: stem cells in neurogenesis, transplantation, and disease modeling. *Brain. Pathol*, **16**, 155–168.
10. Di Giorgio, F.P., Carrasco, M.A., Siao, M.C., Maniatis, T. and Eggan, K. (2007) Non-cell autonomous effect of glia on motor neurons in an embryonic stem cell-based ALS model. *Nat. Neurosci*, **10**, 608–614.
11. Coyle, J.T., Oster-Granite, M.L. and Gearhart, J.D. (1986) The neurobiologic consequences of Down syndrome. *Brain Res. Bull*, **16**, 773–787.
12. Scott, B.S., Becker, L.E. and Petit, T.L. (1983) Neurobiology of Down's syndrome. *Prog. Neurobiol*, **21**, 199–237.
13. Becker, L., Mito, T., Takashima, S. and Onodera, K. (1991) Growth and development of the brain in Down syndrome. *Prog. Clin. Biol. Res*, **373**, 133–152.
14. Schmidt-Sidor, B., Wisniewski, K.E., Shepard, T.H. and Sersen, E.A. (1990) Brain growth in Down syndrome subjects 15 to 22 weeks of gestational age and birth to 60 months. *Clin. Neuropathol*, **9**, 181–190.
15. Wisniewski, K.E. (1990) Down syndrome children often have brain with maturation delay, retardation of growth, and cortical dysgenesis. *Am. J. Med. Genet. Suppl*, **7**, 274–281.
16. Ross, M.H., Galaburda, A.M. and Kemper, T.L. (1984) Down's syndrome: is there a decreased population of neurons? *Neurology*, **34**, 909–916.
17. Weitzdoerfer, R., Dierssen, M., Fountoulakis, M. and Lubec, G. (2001) Fetal life in Down syndrome starts with normal neuronal density but impaired dendritic spines and synaptosomal structure. *J. Neural. Transm. Suppl*, 59–70.
18. Becker, L.E., Armstrong, D.L. and Chan, F. (1986) Dendritic atrophy in children with Down's syndrome. *Ann. Neurol*, **20**, 520–526.
19. Busciglio, J. and Yankner, B.A. (1995) Apoptosis and increased generation of reactive oxygen species in Down's syndrome neurons in vitro. *Nature*, **378**, 776–779.
20. Busciglio, J., Pelsman, A., Wong, C., Pigino, G., Yuan, M., Mori, H. and Yankner, B.A. (2002) Altered metabolism of the amyloid beta precursor protein is associated with mitochondrial dysfunction in Down's syndrome. *Neuron*, **33**, 677–688.
21. Bahn, S., Mimmack, M., Ryan, M., Caldwell, M.A., Jauniaux, E., Starkey, M., Svendsen, C.N. and Emson, P. (2002) Neuronal target genes of the neuron-restrictive silencer factor in neurospheres derived from fetuses with Down's syndrome: a gene expression study. *Lancet*, **359**, 310–315.
22. Ramalho-Santos, M., Yoon, S., Matsuzaki, Y., Mulligan, R.C. and Melton, D.A. (2002) 'Stemness': transcriptional profiling of embryonic and adult stem cells. *Science*, **298**, 597–600.
23. D'Amour, K.A. and Gage, F.H. (2003) Genetic and functional differences between multipotent neural and pluripotent embryonic stem cells. *Proc. Natl. Acad. Sci. USA*, **100** (Suppl. 1), 11866–11872.
24. Ellis, P., Fagan, B.M., Magness, S.T., Hutton, S., Taranova, O., Hayashi, S., McMahon, A., Rao, M. and Pevny, L. (2004) SOX2, a persistent marker for multipotential neural stem cells derived from embryonic stem cells, the embryo or the adult. *Dev. Neurosci*, **26**, 148–165.
25. Graham, V., Khudyakov, J., Ellis, P. and Pevny, L. (2003) SOX2 functions to maintain neural progenitor identity. *Neuron*, **39**, 749–765.
26. Hermanson, O., Jepsen, K. and Rosenfeld, M.G. (2002) N-CoR controls differentiation of neural stem cells into astrocytes. *Nature*, **419**, 934–939.
27. Regad, T., Roth, M., Bredenkamp, N., Illing, N. and Papalopulu, N. (2007) The neural progenitor-specifying activity of FoxG1 is antagonistically regulated by CKI and FGF. *Nat. Cell. Biol*, **9**, 531–540.
28. Corbo, J.C., Deuel, T.A., Long, J.M., LaPorte, P., Tsai, E., Wynshaw-Boris, A. and Walsh, C.A. (2002) Doublecortin is required in mice for lamination of the hippocampus but not the neocortex. *J. Neurosci*, **22**, 7548–7557.
29. Gleeson, J.G., Lin, P.T., Flanagan, L.A. and Walsh, C.A. (1999) Doublecortin is a microtubule-associated protein and is expressed widely by migrating neurons. *Neuron*, **23**, 257–271.
30. Doetsch, F., Caille, I., Lim, D.A., Garcia-Verdugo, J.M. and Alvarez-Buylla, A. (1999) Subventricular zone astrocytes are neural stem cells in the adult mammalian brain. *Cell*, **97**, 703–716.
31. Sanai, N., Tramontin, A.D., Quinones-Hinojosa, A., Barbaro, N.M., Gupta, N., Kunwar, S., Lawton, M.T., McDermott, M.W., Parsa, A.T., Manuel-Garcia Verdugo, J. *et al.* (2004) Unique astrocyte ribbon in adult human brain contains neural stem cells but lacks chain migration. *Nature*, **427**, 740–744.
32. Shin, S., Sun, Y., Liu, Y., Khaner, H., Svant, S., Cai, J., Xu, Q.X., Davidson, B.P., Stice, S.L., Smith, A.K. *et al.* (2007) Whole genome analysis of human neural stem cells derived from embryonic stem cells and stem and progenitor cells isolated from fetal tissue. *Stem Cells*, **25**, 1298–1306.
33. Calvano, S.E., Xiao, W., Richards, D.R., Felciano, R.M., Baker, H.V., Cho, R.J., Chen, R.O., Brownstein, B.H., Cobb, J.P., Tschoeke, S.K. *et al.* (2005) A network-based analysis of systemic inflammation in humans. *Nature*, **437**, 1032–1037.
34. Behar, T.N. and Colton, C.A. (2003) Redox regulation of neuronal migration in a Down Syndrome model. *Free Radic. Biol. Med*, **35**, 566–575.
35. Mazur-Kolecka, B., Golabek, A., Nowicki, K., Flory, M. and Frackowiak, J. (2005) Amyloid-beta impairs development of neuronal progenitor cells by oxidative mechanisms. *Neurobiol. Aging*, **27**, 1181–1192.
36. Schmidt, S. (1998) S100B: pathogenetic and pathophysiologic significance in neurology. *Nervenarzt*, **69**, 639–646.
37. Allore, R., O'Hanlon, D., Price, R., Neilson, K., Willard, H.F., Cox, D.R., Marks, A. and Dunn, R.J. (1988) Gene encoding the beta subunit of S100 protein is on chromosome 21: implications for Down syndrome. *Science*, **239**, 1311–1313.
38. Mrak, R.E. and Griffin, W.S. (2004) Trisomy 21 and the brain. *J. Neuropathol. Exp. Neurol*, **63**, 679–685.
39. Cavazzin, C., Ferrari, D., Facchetti, F., Russignan, A., Vescovi, A.L., La Porta, C.A. and Gritti, A. (2006) Unique expression and localization of aquaporin-4 and aquaporin-9 in murine and human neural stem cells and in their glial progeny. *Glia*, **53**, 167–181.
40. Esposito, G., De Filippis, D., Cirillo, C., Sarnelli, G., Cuomo, R. and Iuvone, T. (2005) The astroglial-derived S100beta protein stimulates the expression of nitric oxide synthase in rodent macrophages through p38 MAP kinase activation. *Life Sci*, **78**, 2707–2715.
41. Reeves, R.H., Yao, J., Crowley, M.R., Buck, S., Zhang, X., Yarowsky, P., Gearhart, J.D. and Hilt, D.C. (1994) Astrocytosis and axonal proliferation in the hippocampus of S100b transgenic mice. *Proc. Natl. Acad. Sci. USA*, **91**, 5359–5363.
42. Griffin, W.S., Sheng, J.G., McKenzie, J.E., Royston, M.C., Gentleman, S.M., Brumback, R.A., Cork, L.C., Del Bigio, M.R., Roberts, G.W. and Mrak, R.E. (1998) Life-long overexpression of S100beta in Down's syndrome: implications for Alzheimer pathogenesis. *Neurobiol. Aging*, **19**, 401–405.
43. Stabel-Burow, J., Kleu, A., Schuchmann, S. and Heinemann, U. (1997) Glutathione levels and nerve cell loss in hippocampal cultures from trisomy 16 mouse–a model of Down syndrome. *Brain Res*, **765**, 313–318.
44. Hebenstreit, D., Horejs-Hoeck, J. and Duschl, A. (2005) JAK/STAT-dependent gene regulation by cytokines. *Drug News Perspect*, **18**, 243–249.
45. Pearson, G., Robinson, F., Beers Gibson, T., Xu, B.E., Karandikar, M., Berman, K. and Cobb, M.H. (2001) Mitogen-activated protein (MAP) kinase pathways: regulation and physiological functions. *Endocr. Rev*, **22**, 153–183.
46. Nesic, O., Lee, J., Ye, Z., Unabia, G.C., Rafati, D., Hulsebosch, C.E. and Perez-Polo, J.R. (2006) Acute and chronic changes in aquaporin 4 expression after spinal cord injury. *Neuroscience*, **143**, 779–792.
47. Nesic, O., Lee, J., Johnson, K.M., Ye, Z., Xu, G.Y., Unabia, G.C., Wood, T.G., McAdoo, D.J., Westlund, K.N., Hulsebosch, C.E. *et al.* (2005)

Transcriptional profiling of spinal cord injury-induced central neuropathic pain. *J. Neurochem*, **95**, 998–1014.
48. Henzler, T. and Steudle, E. (2000) Transport and metabolic degradation of hydrogen peroxide in Chara corallina: model calculations and measurements with the pressure probe suggest transport of H(2)O(2) across water channels. *J. Exp. Bot*, **51**, 2053–2066.
49. Nicchia, G.P., Frigeri, A., Liuzzi, G.M. and Svelto, M. (2003) Inhibition of aquaporin-4 expression in astrocytes by RNAi determines alteration in cell morphology, growth, and water transport and induces changes in ischemia-related genes. *Faseb J*, **17**, 1508–1510.
50. Lyle, R., Gehrig, C., Neergaard-Henrichsen, C., Deutsch, S. and Antonarakis, S.E. (2004) Gene expression from the aneuploid chromosome in a trisomy mouse model of Down syndrome. *Genome Res*, **14**, 1268–1274.
51. Coates, P.J., Lorimore, S.A. and Wright, E.G. (2005) Cell and tissue responses to genotoxic stress. *J. Pathol*, **205**, 221–235.
52. Hagberg, H. and Mallard, C. (2005) Effect of inflammation on central nervous system development and vulnerability. *Curr. Opin. Neurol*, **18**, 117–123.
53. Mao, R., Zielke, C.L., Zielke, H.R. and Pevsner, J. (2003) Global up-regulation of chromosome 21 gene expression in the developing Down syndrome brain. *Genomics*, **81**, 457–467.
54. Mao, R., Wang, X., Spitznagel, E.L., Jr, Frelin, L.P., Ting, J.C., Ding, H., Kim, J.W., Ruczinski, I., Downey, T.J. and Pevsner, J. (2005) Primary and secondary transcriptional effects in the developing human Down syndrome brain and heart. *Genome Biol*, **6**, R107.
55. Amano, K., Sago, H., Uchikawa, C., Suzuki, T., Kotliarova, S.E., Nukina, N., Epstein, C.J. and Yamakawa, K. (2004) Dosage-dependent expression of genes in the trisomic region of Ts1Cje mouse model for Down syndrome. *Hum. Mol. Genet*, **13**, 1333–1340.
56. Dauphinot, L., Lyle, R., Rivals, I., Dang, M.T., Moldrich, R.X., Golfier, G., Ettwiller, L., Toyama, K., Rossier, J., Personnaz, L. *et al.* (2005) The cerebellar transcriptome during postnatal development of the Ts1Cje mouse, a segmental trisomy model for Down syndrome. *Hum. Mol. Genet*, **14**, 373–384.
57. FitzPatrick, D.R., Ramsay, J., McGill, N.I., Shade, M., Carothers, A.D. and Hastie, N.D. (2002) Transcriptome analysis of human autosomal trisomy. *Hum. Mol. Genet*, **11**, 3249–3256.
58. Tang, Y., Schapiro, M.B., Franz, D.N., Patterson, B.J., Hickey, F.J., Schorry, E.K., Hopkin, R.J., Wylie, M., Narayan, T., Glauser, T.A. *et al.* (2004) Blood expression profiles for tuberous sclerosis complex 2, neurofibromatosis type 1, and Down's syndrome. *Ann. Neurol*, **56**, 808–814.
59. Saran, N.G., Pletcher, M.T., Natale, J.E., Cheng, Y. and Reeves, R.H. (2003) Global disruption of the cerebellar transcriptome in a Down syndrome mouse model. *Hum. Mol. Genet*, **12**, 2013–2019.
60. Cecil, D.L., Johnson, K., Rediske, J., Lotz, M., Schmidt, A.M. and Terkeltaub, R. (2005) Inflammation-induced chondrocyte hypertrophy is driven by receptor for advanced glycation end products. *J. Immunol*, **175**, 8296–8302.
61. Lam, A.G., Koppal, T., Akama, K.T., Guo, L., Craft, J.M., Samy, B., Schavocky, J.P., Watterson, D.M. and Van Eldik, L.J. (2001) Mechanism of glial activation by S100B: involvement of the transcription factor NFkappaB. *Neurobiol. Aging*, **22**, 765–772.
62. Papadopoulos, M.C., Krishna, S. and Verkman, A.S. (2002) Aquaporin water channels and brain edema. *Mt. Sinai J. Med*, **69**, 242–248.
63. La Porta, C.A., Gena, P., Gritti, A., Fascio, U., Svelto, M. and Calamita, G. (2005) Adult murine CNS stem cells express aquaporin channels. *Biol. Cell*.
64. Badaut, J., Lasbennes, F., Magistretti, P.J. and Regli, L. (2002) Aquaporins in brain: distribution, physiology, and pathophysiology. *J. Cereb. Blood Flow Metab*, **22**, 367–378.
65. Venero, J.L., Vizuete, M.L., Machado, A. and Cano, J. (2001) Aquaporins in the central nervous system. *Prog. Neurobiol*, **63**, 321–336.
66. Griesdale, D.E. and Honey, C.R. (2004) Aquaporins and brain edema. *Surg. Neurol*, **61**, 418–421.
67. Ma, T., Yang, B., Gillespie, A., Carlson, E.J., Epstein, C.J. and Verkman, A.S. (1997) Generation and phenotype of a transgenic knockout mouse lacking the mercurial-insensitive water channel aquaporin-4. *J. Clin. Invest*, **100**, 957–962.
68. Manley, G.T., Fujimura, M., Ma, T., Noshita, N., Filiz, F., Bollen, A.W., Chan, P. and Verkman, A.S. (2000) Aquaporin-4 deletion in mice reduces brain edema after acute water intoxication and ischemic stroke. *Nat. Med*, **6**, 159–163.
69. Kola, I. and Hertzog, P.J. (1998) Down syndrome and mouse models. *Curr. Opin. Genet. Dev*, **8**, 316–321.
70. O'Doherty, A., Ruf, S., Mulligan, C., Hildreth, V., Errington, M.L., Cooke, S., Sesay, A., Modino, S., Vanes, L., Hernandez, D. *et al.* (2005) An aneuploid mouse strain carrying human chromosome 21 with Down syndrome phenotypes. *Science*, **309**, 2033–2037.
71. Sohn, S.Y., Weitzdoerfer, R., Mori, N. and Lubec, G. (2003) Transcription factor REST dependent proteins are comparable between Down syndrome and control brains: challenging a hypothesis. *J. Neural. Transm. Suppl*, 59–66.
72. Sheen, V.L. and Macklis, J.D. (1995) Targeted neocortical cell death in adult mice guides migration and differentiation of transplanted embryonic neurons. *J. Neurosci*, **15**, 8378–8392.
73. Sheen, V.L., Wheless, J.W., Bodell, A., Braverman, E., Cotter, P.D., Rauen, K.A., Glenn, O., Weisiger, K., Packman, S., Walsh, C.A. *et al.* (2003) Periventricular heterotopia associated with chromosome 5p anomalies. *Neurology*, **60**, 1033–1036.
74. Wright, L.S., Li, J., Caldwell, M.A., Wallace, K., Johnson, J.A. and Svendsen, C.N. (2003) Gene expression in human neural stem cells: effects of leukemia inhibitory factor. *J. Neurochem*, **86**, 179–195.
75. Tusher, V.G., Tibshirani, R. and Chu, G. (2001) Significance analysis of microarrays applied to the ionizing radiation response. *Proc. Natl. Acad. Sci. USA*, **98**, 5116–5121.
76. Sun, T., Patoine, C., Abu-Khalil, A., Visvader, J., Sum, E., Cherry, T.J., Orkin, S.H., Geschwind, D.H. and Walsh, C.A. (2005) Early asymmetry of gene transcription in embryonic human left and right cerebral cortex. *Science*, **308**, 1794–1798.
77. Mihara, M. and Uchiyama, M. (1978) Determination of malonaldehyde precursor in tissues by thiobarbituric acid test. *Anal. Biochem*, **86**, 271–278.
78. Mosmann, T. (1983) Rapid colorimetric assay for cellular growth and survival: application to proliferation and cytotoxicity assays. *J. Immunol. Methods*, **65**, 55–63.